TÉCNICO LISBOA

Reaction Calorimetry and Thermodynamic & Kinetic Modelling Towards a faster Chemistry Development

Mariana Casquilha Castelo Pereira

Thesis to obtain the Master of Science Degree in

Biological Engineering

Supervisors: Dr. Filipe André Prata Ataíde
Prof. Dr. Francisco Manuel da Silva Lemos

Examination Committee

Chairperson: Prof. Dr. Helena Maria Rodrigues Vasconcelos Pinheiro
Supervisor: Dr. Filipe André Prata Ataíde
Members of the Committee: Prof. Dr. Carlos Manuel Faria de Barros Henriques
Nuno Lousa Pereira

October 2021

I declare that this document is an original work of my own authorship and that it fulfills all the requirements of the Code of Conduct and Good Practices of the Universidade de Lisboa.

Preface

The work presented in this thesis was performed at the Process Chemistry Development Group of Hovione (Lisbon, Portugal), during the period October 2020-March 2021, under the supervision of Dr. Filipe Ataide. The thesis was co-supervised at Instituto Superior Técnico by Prof. Francisco Lemos.

Acknowledgments

I would like to thank my parents, Sandra e Sérgio, for their encouragement and for believing in me more than I do. To my (not so) little sisters, Carolina and Margarida, to whom I hope to represent an example and a friend. To my four grandparents, Maria do Carmo, Natália, Ernesto and José Manuel, who always appreciated my effort and cared about me. I admire you all and I am blessed to have all of you in my life.

I am very grateful to Hovione for the opportunity, specially to Dr. Filipe Ataide for his sympathy, tireless dedication, and sharing of knowledge.

I would like to acknowledge Prof. Dr. Francisco Lemos for his attendance, insight, wisdom, and great inspiration.

Without Dr. Filipe and Prof. Francisco this thesis would not be possible.

I would also like to thank Prof. Dr. Amélia Lemos for her contribution.

To all my friends and colleagues that helped me grow as a person and were always there for me through the challenging times of the academic path, with a special thanks to Margarida, for her comprehension and unconditional support, to Sofia for her great generosity and joy, and David for his engaging curiosity and specifically for sharing the project weightiness with me.

To my childhood friends, specially to Mariana who I have grown up with, thank you for your sympathy, empathy and generosity and to Carla for always being there for me.

Last but not least, thank you, Guilherme for the support, love, understanding and for making the weekends feel short.

To each and every one of you – Thank you.

Abstract

The present work is in the scope of chemical process development in the pharmaceutical industry and fine chemistry. The pharmaceutical industry has been shifting to a predictive process development industry. However, there is still a lack of information on chemical systems in the early stages of the process development. Besides, some analytical tools in use do not suit the industry needs on the required information in an expedited manner.
In this work, it is presented a systematic study on how to use isothermal reaction calorimetry to address kinetic and thermodynamic reaction modelling, with the final purpose of predicting the reaction scale-up. This study is focused on simple mechanisms: first order 1 and consecutive 2-step mechanisms. After generating simulated calorimetry and concentrated data, several modelling experiments were performed.
This study demonstrates the potential of using data from reaction calorimetry on chemical process optimization and scale-up. From the present work it was possible to suggest recommendations for a preliminary methodology to use calorimetric data as a tool for kinetic and thermodynamic modelling towards a faster chemical development: (1) the use of at least 2-runs of the reaction at two different temperatures, (2) how to combine calorimetry data with on-line concentration data and (3) pre-fitting of the model to the data before iterative estimation.

Keywords

Kinetics; Thermodynamics; Modelling; Reaction Calorimetry.

Resumo

Este trabalho encontra-se no âmbito do desenvolvimento de processos químicos na indústria farmacêutica. Apesar do paradigma desta indústria estar a mudar no sentido de prever o processo, ao invés de o testar iterativamente, existem lacunas na informação existente sobre os sistemas reacionais nas fases preliminares do desenvolvimento de processo. Para além disso, algumas das técnicas analíticas usadas não servem as necessidades da indústria em relação à geração da informação necessária em tempo útil.

Neste trabalho, é apresentado um estudo sistemático que pretende analisar como usar calorimetria de reação para o estudo cinético e termodinâmico de reações químicas. Depois de se gerarem dados de calorimetria e concentração simulados, várias experiências de modelação foram realizadas. As reações estudadas prendem-se com mecânismos simples compostos por 1 ou 2 passos consecutivos de primeira-ordem.

Este estudo demonstra o potencial da calorimetria de reação aplicada à optimização de reações químicas e o seu *scale-up*. Através deste estudo foi possível sugerir recomendações para uma metodologia preliminar incluindo dados calorimétricos como ferramenta de modelação cinética e termodinâmica: (1) uso de pelos menos dois ensaios isotérmicos a duas temperaturas diferentes, (2) como usar dados calorimétricos combinados com dados de concentração (3) pré-ajuste do modelo aos dados experimentais antes de proceder ao calculo iterativo.

Palavras Chave

Modelação; Cinética; Termodinâmica; Calorimetria de Reação.

Contents

List of Figures

List of Tables

Nomenclature

Chemical Constants

R	Molar Gas Constant	8.314 J mol^{-1} K^{-1}

Variables

ΔH_r	Reaction enthalpy	J mol^{-1}
Δt	Time span	min^{-1}
$\dot{m}$	mass flow rate	W
$\dot{q}$	Heat rate	W
μ	Mean	
σ	Standard deviation	
σ^2	Variance	
A	Heat transfer area	m^2
C	Concentration	mol L^{-1}
Cp	Specific heat capacity	J kg^{-1} K^{-1}
Ea	Activation energy	J mol^{-1}
k^{1st}	First order kinetic constant	min^{-1}
k^{2nd}	Second order kinetic constant	L mol^{-1} s^{-1}
k_0	Pre-exponential factor	
m	Mass	kg

Q_v	Volumetric flow rate	mL min^{-1}
r	Reaction rate	mol L^{-1} min^{-1}
s	Signal	
T	Temperature	
U	Overall heat transfer coefficient	W m^{-2} K^{-1}
V	Volume	

Acronyms

API Active Pharmaceutical Ingredient

DC DynoChem

FTIR Fourier Transform Infrared Spectroscopy

GMP Good Manufacturing Practices

HPLC High Performance Liquid Chromatography

IR-ATR Infrared Attenuated Total Reflectance

NIR Near Infrared

PAT Process Analytic Technology

QbD Quality by Design

R&D Research and Development

Sub and Superscripts

0	initial
ac	accumulation
ap	apparent
f	final
$flow$	jacket flow

i	step number
in	inlet
j	jacket
$loss$	dissipated
r	reactor
ref	reference

1

Introduction

Contents

1.1 Context and Motivation

The scope of this work is pharmaceutical integrated process development. Such process development comprises chemical, economic and sustainability as its aspects [2]. The present work will focus on the core stage of the chemical process development: the chemical reaction, although bearing the other two in mind. The chemical reaction step development aims to optimize the chemical transformation, which if successful in this endeavour will generate a good contribution to the economic, ecologic and safety aspects of the development. In fact, «improving the reaction step is an important task of an integrated process development and has a crucial effect on the overall performance of the production process» [1].

Thus, a good reaction optimization results in a set of conditions where the main product is favoured and unwanted by-products are minimized, in other words, conditions for the reaction to be conducted that assure high yield and purity. Therefore, it will also result in higher profitability and less waste, contributing to the economic and sustainable aspects of the process development. To extend these advantages, the chemical optimization should start in the early stages of the process [1].

To that end, it is required to fill the lack of information on chemical reactions, in the initial stages of the process development. This knowledge is essential to expedite reaction optimization with the final aim of its scale-up. The purpose of this thesis to address this issue, using reaction calorimetry tools for kinetic and thermodynamic modelling of pharmaceutical chemical systems.

1.2 Pharmaceutical Industry and Kinetic Modelling

In the pharmaceutical industry, there is a consistent need to ensure that clinical supplies are manufactured and delivered on time. On the other hand, manufacturers are constantly facing with the question of the best use of the limited financial resources available. Besides, in this context, process development, optimization and scale-up historically tend to be an iterative approach. This approach entails time and high costs/wastes, therefore, the industry has been shifting toward predictability from lab to production [3, 4].

Aside from the importance of time to market and cost-effectiveness specific needs related to the pharmaceutical industry, it is also required to agree with GMP (Good Manufacturing Practices) and PAT (Process Analytic Techniques) – A Framework for Innovative Pharmaceutical Manufacturing and Quality Assurance. This guidance reflects the new thinking mode of the industry concerning the quality assessment: which is turning to be a design subject – Quality by Design (QbD) – instead of final product parameters [5, 6]. These principles currently leading the industry are accompanied by novel techniques to be applied in the process development that gives primacy to continuous and fast monitoring and control.

In 2010, Troup and Georgakis questioned some of the major american pharmaceutical companies about the primary measurement system applied to reaction monitoring for API production. The main answer was in-line Mid Infrared spectroscopy. Other techniques such as in-line Raman spectroscopy, in-line NIR, and on-line HPLC were also comprised. During process development, the concentration profiles measured from the tools listed above are used to determine reaction mechanisms, identification of reaction intermediates, and kinetic rate parameters for modelling [7].

Thus, there are many powerful analytical tools available for chemical identification and quantification already in use for modelling purposes, although their use on/in-line may be a path in development for smaller companies, especially in this context.

In these circumstances, some of the existing in-use techniques are time-consuming, especially if calibration and sampling is needed (e.g. HPLC), others do not reveal the required information especially if the reaction is fast. Besides, some of these techniques require sophisticated mathematical knowledge to determine the parameters [1] At last, some of the techniques in use require sampling in a particular form that may not correspond to the original matrix [8].

Apart from the previously referred technical issues, there are strategic obstacles. First, the chemical systems applied in pharmaceuticals are quite complex. Second, the process optimization still lacks investment, remaining a second class activity which may result in insufficient experiments [1, 4].

All things considered, to transform a conservative industry into a predictive process design industry to meet the timely, economic, sustainability and regulatory goals, requires continuous improvement in scientific and technical tools as well as multidisciplinary skill sets in the R&D labs, including chemical engineering science. Chemical engineering principles are adequate to help address these needs in part derived from the skill to predict using mathematical models and their understanding of equipment and manufacturability, helping transform the pharmaceutical industry from an industry focusing on inventing and testing to a process and product design industry [4].

The present thesis lies on the kinetic and thermodynamic modelling to expedite the chemical reaction process design with a view of scaling up a fed-batch reaction operation.

1.3 Kinetic modelling and Reaction Calorimetry

Process development and chemical reaction optimization depend on an appropriate reaction model. For a large number of pharmaceutical reactions, such models are not available or it is difficult to develop within the available time [9]. Despite it, it should be possible to describe the majority of the chemical reactions using an empirical model that describes the main and side reactions, with a minimum number of reactions parameters [9, 10].
A standard analytical tool for kinetic and thermodynamic modelling is reaction calorimetry [1, 10–16].

As previously mentioned, there are many analytical tools to follow the reaction kinetics, however, calorimetry (measurement of the heat flow) implies that both kinetic and thermodynamics contribute to the observed signal, including phase changes and heat and mass transfer phenomena [17].
Reaction calorimetry requires conducting an energy balance to the semi-batch reactor – eq. (1.1) [18]. In a fed-batch reactor, the accumulated heat energy ($\dot{q}_{ac}$, W) is equal to the sum of all heat transfer sources: the jacket ($\dot{q}_{flow}$), the reaction ($\dot{q}_r$) and the feed ($\dot{q}_{in}$).

$$\begin{aligned}\dot{q}_{ac} &= \dot{q}_{flow} + \dot{q}_r + \dot{q}_{in} \\ &= m\,Cp\,\frac{dT_r}{dt} = U\,A\,(T_j - T_r) + r\,V(t)\,\Delta H_r + \dot{m}\,Cp\,(T^{in} - T_r) \quad (1.1)\end{aligned}$$

Where, $m, Cp, T_r, U, A, T_j, r, V, \Delta H_r, \dot{m}, T^{in}$ are reaction mixture mass, reaction mixture heat capacity, reactor temperature, overall heat-transfer coefficient, heat-transfer area, jacket temperature, reaction rate, reactor volume, reaction enthalpy, inlet mass flow rate, inlet stream heat capacity and the temperature of inlet stream, respectively.
If there is another tangible heat phenomenon (as mass or heat transfer) the respective terms should be included in the balanced equation. In this case, only homogeneous reaction systems will be addressed, with negligible enthalpies of mixing.

As the Equation (1.1) suggests, the reactor heat transfer capacity has to be characterized (Equation (1.1)). The heat transfer characterization may be through experimental determination (solvent test) or estimated by modelling to the data (without the reaction) [13] or even using empirical equations [19]. $\dot{q}_f low$ is specially important in the large scale reactor (see Section 1.4)

The reaction rate depends on kinetic constant(s) linked to the mechanism at hand. The kinetic constant dependence with the temperature is expressed with Arrhenius equation – eq. (1.2).

$$k = k_0\, e^{-\frac{Ea}{RT}} \tag{1.2}$$

Where k, k_0, Ea, R, T represent kinetic constant[1], the pre-exponential factor[1], activation energy (J K^{-1}), gas constant (J mol^{-1} K^{-1}) and temperature (K), respectively.
The heat balance shows mathematically the dependence of the kinetic and thermodynamic reaction behaviour on the heat signal.

As the heat flow rate during a chemical reaction is proportional to the rate of conversion, calorimetry represents a differential kinetic analysis method (eq. (1.3)) [11]:

$$\dot{q}_r(t) \propto r(t)V \tag{1.3}$$

This relation implies that subtle changes in concentration profiles may be magnified in heat flow measurements.

In contrast to calorimetry, other analytical techniques applied in this context, such as concentration measurements, online measurements of reaction spectra (see 1.2) can be compared to an integral kinetic analysis methods: the signal/measurements (s_i) obtained by them are proportional to the concentration profiles ($C_i(t)$) in mol L^{-1} – eq. (1.4)).

[1] Kinetics dependent units

$$s_i(t) \propto C_i(t) \tag{1.4}$$

This is why it has been endorsed that combinations of both calorimetry and integral kinetic analysis techniques lead to a significant improvement on the kinetic analysis [1, 9–11, 18, 20, 21].

Reactions involved in API synthesis are often followed by significant heat release, therefore they must be truly understood to be properly managed on a factory scale, as thermal instability and explosive behaviour can be extremely destructive and costly events [22]. Reaction calorimetry can help to predict the likely behaviour of chemicals when reactions, transport and storage are concerned [8].

In fact, reaction calorimetry plays a crucial role on safety assessments and parameter determination, as activation energies and enthalpy of reaction, heat capacities and even kinetic constants [14, 15, 23–26].

1.4 Reaction Calorimetry and Safety Assessment

Pharmaceutical reaction operations are often conducted in batch/semi-batch mode [4]. Although batch and semi-batch reactors are versatile, they entail some disadvantages that may compromise the process safety, such as product and heat accumulation.

For the reasons previously stated, when the chemical transformation is overall exothermic, it is advantageous to conduct it in fed-batch mode. While in a true batch reactor all the reactants are initially charged in the reactor, the semi-batch reactor allows controlling the course of the reaction not only by the temperature but also by the feed flow rate. The additional parameter available to control is not only useful for safety matters but also may influence the quality, in particular, the selectivity of a reaction [23].

Therefore, a general approach of a safety assessment for a semi-batch reactor in the frame of scale-up includes: (1) the set of the conditions where the heat of the reaction can be removed by the cooling system of the reactor and (2) which temperature can be reached in case of a cooling failure/what are the consequences [23].
This work will only approach topic (1), which is directly related to the optimization of the scale-up operation in safe conditions. Further studies which take in consideration the system behaviour in case of failure are out of the scope of this work.

Regarding the reactor behaviour in normal conditions, *i.e.* the control of the reaction rate, one important parameter is heat accumulation, ($\dot{q}_{ac}$) [27]. The heat accumulation «represents the variation of the energy of the content with the temperature» [28]. For a semi-batch reactor, if the heat exchange does not compensate the heat of the reaction ($\dot{q}_r$) and the thermal effect of the feed ($\dot{q}_{flow}$), then the reactor temperature will change. Hence, the heat accumulation depends on the reaction rate, the feed rate as well as the reactor heat removal, see eq. (1.1).

For fast reactions, since the added reactant is immediately converted to the product, no significant accumulation of the added reactant occurs and the rate of reaction is limited by the rate of addition. With slower reactions, the compound fed to the reactor does not immediately react away, leading to accumulation – kinetics control the reaction rate. In these cases, it is crucial to extend the feed time, decreasing the feed rate, in order to limit reactants accumulation, that when reacting release energy – dosing controlled reaction [28].

1.5 Reaction Calorimetry Fundamentals

As discussed above, calorimetry is a convenient tool to study reaction kinetic and thermodynamic behaviour. In this section, the main fundamentals of reaction calorimetry sustaining this work will be presented. As the finality of the modelling work is the scale-up of the reaction, only calorimeters that resemble the production scale (batch/semi-batch reactors) are applicable.

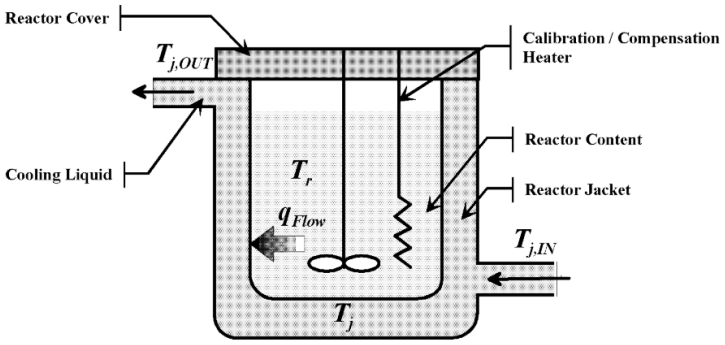

Figure 1.1: Heat flow general scheme, where $\dot{q}_{flow}$ refers to the heat removed by the jacket, expressing the control dynamics of an heat-flow calorimeter, *Zogg et al. 2003* [1].

Regarding the operation mode, this work will be focused on isothermal measurements, therefore no other operational modes will be discussed (adiabatic, isoperibole, etc). Although further operation modes could be useful according to the final purpose, the isothermal operation mode is considered to be the easiest to apply. Since there is no change on Tr it is not necessary to take heat accumulation in the reactor content into account – see eq. (1.1). Note that if there is a subtle change it is driven by non-idealities. Operating in such mode simplifies the heat balance, eq. (1.1), $\dot{q}_{ac} = 0$. Thus, no reaction $Cp\,(T_r)$ calculation is required [11].

There are different types of reaction calorimeters. Most of them consist of a reaction vessel with a surrounding jacket with a circulating fluid [11], as Figure 1.1 illustrates. Such devices can be classified according to their measurement and control principles into the following four categories: heat-flow calorimeter, power-compensation reaction calorimeter, heat-balance reaction calorimeter and Peltier calorimeters. The four measurement/control principles had already been described in literature [1, 11, 13, 14, 17]. In the present work, the calorimeter in use follows the heat flow principle: T_r is controlled by varying the temperature of the cooling liquid, T_j – Figure 1.1.

1.6 Thesis Objectives and Alignment

The focus of this work is to include calorimetry data provided by a Metller Toledo RC1 [29] (a heat-flow calorimeter already in use for safety assessments) in the chemical development, to accomplish a more comprehensive knowledge on the kinetics and thermodynamics of the pharmaceutical reactions, in the early stages of chemical development.

The main purpose of this work is to contribute to a methodology in which the aim is to use reaction calorimetry data for kinetic and thermodynamics modelling of chemical reactions, with a final purpose of safe and optimal scale-up.

In order to demonstrate the purpose of this thesis a case study will be presented Chapter 2, followed by a systematic study on the impact of different experiments on the modelling results (Chapter 4) using simulated data – see data generator (Chapter 3). The subsequent conclusions and recommendations will be presented in Chapter 5.

2

Case Study

Contents

The first approach to the thesis issue was based on studying a widely known reaction in order to understand the potential of reaction calorimetry in kinetic and thermodynamic modeling. In this chapter, the case study will be presented, as an introduction to the thesis theme and its final aim.

2.1 Acetic Anhydride Hydrolysis

The present case study deals with the acetic anhydride hydrolysis, which according to Andreas Zogg [1], represents a standard reference in reaction calorimetry. In fact, many authors studied this reaction kinetics, at least since 1912 when Orton and Jones published their study using titration to follow the reaction extent [30]. Ever since, several other techniques have been used for this purpose such as conductivity, colorimetry, calorimetry, temperature scanning, or spectroscopic techniques [31].

This extensively studied reaction has been acknowledged as a three step mechanism: one first slow step, an addition, followed by an elimination step and a proton transfer equilibrium [32]. Since the first step is the rate controlling step, it is often described as a concerted first-order reaction [33].

In the present work, Zogg's experimental data were used to build the kinetic model of this reaction [1]. In other words, to estimate the kinetic and thermodynamic parameters with the final aim of predicting the scale-up in optimal conditions.

Andreas Zogg developed a combined approach using calorimetry and IR-ATR (Infrared-Attenuated Total Reflectance) for kinetic and thermodynamic parameters of exothermic reactions [1, 11]. During his work, the new methodology was tested while performing the acetic anhydride hydrolysis reaction in fed-batch mode, at three different temperatures (25, 40, 55 ºC) in which an acetic anhydride and acetic acid mixture (334:277 g) is added (5 mL/min) to 35 mL HCl solution (0.1N). The experiments were monitored by isothermal reaction calorimetry and on-line IR spectroscopy (further experimental details can be checked in Appendix E.2.1. of Ref [1]). Hence, the heat rate and concentration data along the reaction extension were conceivable to use in this work. However, in this work, it was assumed there was no HCl in the reactor, as an approximation, since HCl does not participate in the reaction mechanism.
It is worth noting these experiments were chosen of all the available in the literature to meet the goal of the thesis, concerning the desired techniques to implement in the final methodology.

The DynoChem® model of second-order single-step reaction was used to fit the experimental data to the kinetic model, where acetic anhydride reacts with water to give 2 molecules of acetic acid (Equation (3.1)).

$$\mathrm{AcOAc} + \mathrm{H_2O} \xrightarrow{\mathrm{k^{2nd}},\, \Delta \mathrm{H}_r} 2\,\mathrm{AcOH} \tag{2.1}$$

The balance equations are presented below (eqs. (2.2) to (2.4)).

$$\frac{d(V\,C_{AcOAc})}{dt} = Q_v\,{C_{AcOAc}}^{\mathrm{in}} - k\,C_{AcOAc}(t)\,C_{H_2O}(t)\,V(t) \tag{2.2}$$

Where C_{AcOAc} represents acetic anhydride concentration (M), V the volume (L), Qv represents the feed flow rate (L s^{-1}), k^{2nd} represents the second order reaction rate (L mol^{-1} s^{-1}) and C_{H_2O} represents water concentration (M). In this case, the reaction was not simplified to a pseudo first-order reaction, however kinetic constant conversion is given by $k^{ap} = k^{2nd} \times C_{H_2O}(t)$. Since the water is in excess, its concentration can considered to be constant, after the feeding ($C^f_{H_2O} = 54M$).

$$\frac{dC_{AcOH}}{dt} = 2\,k^{2nd} V(t)\,C_{AcOAc}(t)\,C_{H_2O}(t) \tag{2.3}$$

Where the concentration of acetic acid (C_{AcOH}, M) is given by its formation rate law.

$$\dot{q}(t) = \dot{q}_r(t) = -\Delta H_r \, 2 \, k^{2nd} \, V C_{AcOAc}(t) \, C_{H_2O} \tag{2.4}$$

Where the total heat ($\dot{q}$, W) is equal to reaction heat ($\dot{q}_r$, W), which is given by the heat enthalpy of the reaction ΔH_r multiplied by reaction rate law. The heat of the reaction should be approximately the heat signal of the calorimeter, because the available data had already been treated (baseline corrected) to avoid any other heat phenomena interference, for instance, ($\dot{q}_{in}$). The pre-treatment of the data is carefully described by the author [1].

The algorithm finds the best result while minimizing the error between the model and the experimental data, for all the experiments. The fitting results are presented in Figure 2.1.

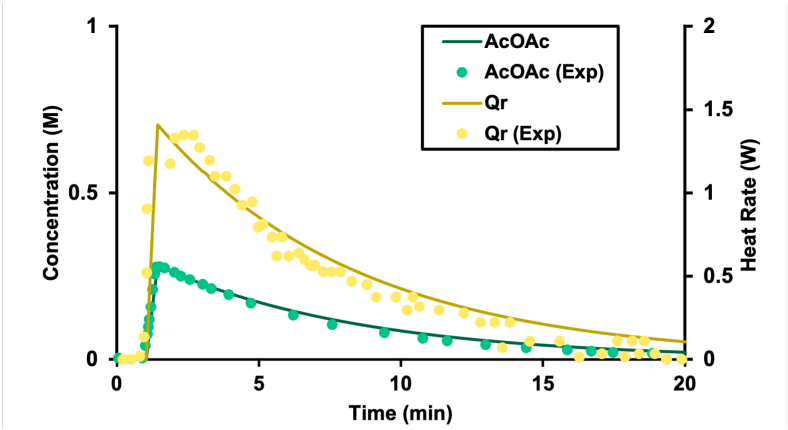

(a)

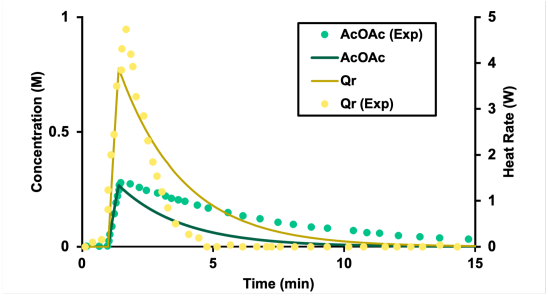

(b)

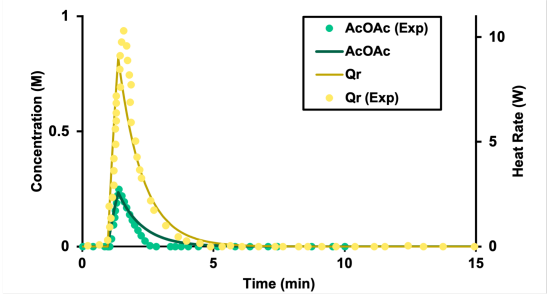

(c)

Figure 2.1: Model results against Zogg's experimental data: AcOAc concentration and Heat Rate, (a) at 25 °C, (b) at 40 °C and (c) at 55 °

According to the Figure 2.1, it is possible to see the model is not perfectly fitted to the experiments, although there is a good agreement between the data and the model. This could be partially explained by a mixing phenomenon between AcOAc/AcOH and water, which was not accounted for in this work, but it was mentioned by the author [1]. In this case, it is a difficult task to conjecture further possible explanations, since the experiments were not carried out during this work.
The analytical results are presented against some of the literature results (see Table 2.1)

Table 2.1: Acetic anhydride hydrolysis: Kinetic and thermodynamic analytical results of the modelling experiment against literature results.

Reference	**Experimental Method**	**Parameter**			
		Ea (kJ mol^{-1})	$ln(k_0)$	k_0 unit	ΔHr (kJ mol^{-1})
This work	Calorimetry + FTIR	55.2	12.2	L mol^{-1} s^{-1}	-57.9
Zogg, 2003 [1]	Calorimetry + FTIR	55.8	16.6	s^{-1}	-60
Asprey et al., 1996 [33]	Conductivity	41.84	7.7	L mol^{-1} s^{-1}	N.D.[1]
Susanne et al., 2012 [32]	NMR	46.02	8.0	L mol^{-1} s^{-1}	N.D.[1]
Hirota et al., 2010 [31]	Temperature Scanning	71	16.8	L mol^{-1} s^{-1}	N.D.[1]
Garcia-Hernandez et al.,2019 [12]	Temperature Scanning	42.1	5.5	L mol^{-1} s^{-1}	N.D.
André et al.,2003 [15]	Calorimetry	N.D.	N.D.	N.D.	-57.9

N.D. - Not Determined

The fitting results agree with the published results, in the sense that the values were found to be in the same range as the ones previously determined, see Table 2.1.

For a direct comparison of this work with Zogg's, the kinetic constants results were converted to k^{ap}. After the conversion, $ln(k^{ap}) = 16.2$ (in opposition to Zogg's 16.6). As it was expected, this work results are closer to Ref. [1] results, when compared with further references. The experiments used were the same, even though the model proposed was not the same, since the heat of solvation was not taken into account in this work, neither HCl presence.
Furthermore, it is interesting to verify that calorimetry experiments used separately, by Hirota [31], resulted in higher values of Ea and $ln(k_0)$ than the combined approach. On another hand, Asprey and Susanne results which do not take the heat phenomena into account seem to be sub-estimated when compared with the combined ones [32, 33].

Overall, the combined approach of the differential and integral methods, as explained in Section 1.3, seem to bring advantages on the estimation of the parameters (although Ref [12] outcome do not follow the premise). However, it is crucial to know how to combine the two [11]. The most significant advantage of the reaction calorimetry approach is the ΔH_r determination. One important parameter that is not possible to estimate through conductivity or spectroscopic techniques. This parameter was successfully calculated when compared with Refs. [1, 15].

With this experiment, the methodology used for kinetic modeling of a first-order reaction is proved to be successful. Also, it shows that more complex mechanisms, as already been proposed [12, 32] could be successfully described through a simpler empirical model, as this is.
This modeling experiment is also suggesting the need to combine one differential method with reaction calorimetry for a comprehensive understanding of the reaction mechanism and thermodynamics, during the same study.

Withal, the model was considered accurate enough to predict the reaction scale-up. The scale-up of the reaction was predicted to be in a fed-batch reactor with 2500 L of working volume.

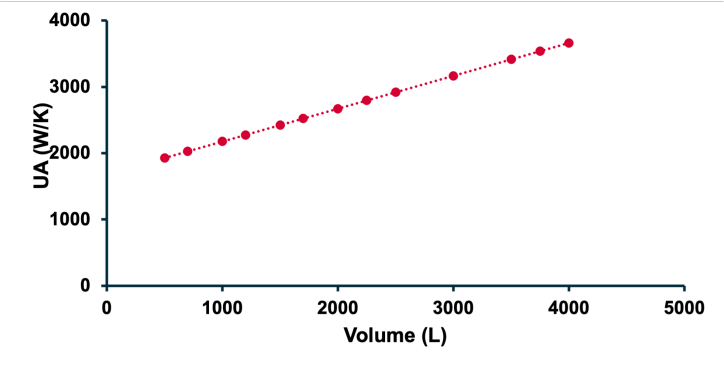

Figure 2.2: Heat transfer capacity of the reactor – represented by $U\,A$ – against the reactor working volume. U was considered to be constant with the volume, the wet area, A, was calculated based on the reactor geometry: $U\,A$ (W/K) = 0.495 Volume (L) + 1681.

The concentration of AcOAc and water was kept equal to the experimental conditions in the lab scenario, proposed by Zogg [1] and described above.

To predict the scale-up of the reaction operation, the reactor heat transfer capacity needs to be characterized. However, in this case, there were no solvent test available, see Section 1.3. Therefore, the overall heat transfer coefficient of the reactor was considered to be constant with the varying volume, and it was estimated based on an experimentally determined value of the $U\,A$ for 1500 L, considering the reactor geometry. The resulting relation between the volume and $U\,A$ is presented in Figure 2.2.

Hence, assuming $U\,A$ corresponding to 2500 L of the production scale reactor is approximately 2918.8 W/K, the reaction operation scaled up was predicted in several scenarios, corresponding to different conditions.

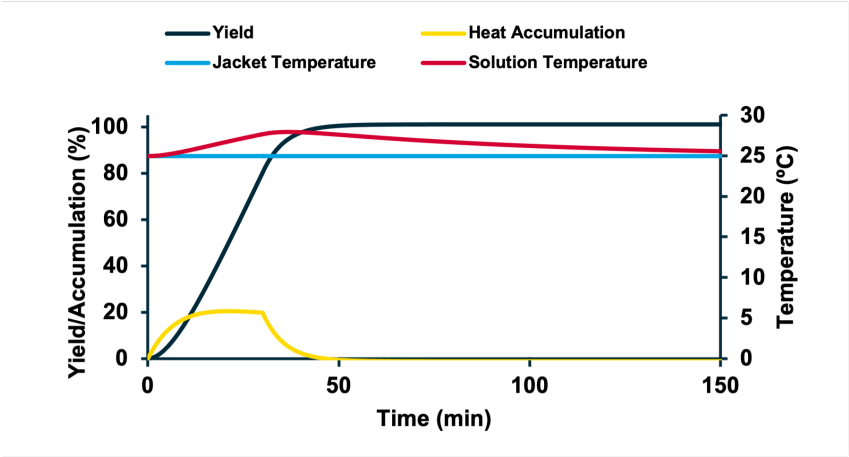

Figure 2.3: Scale up prediction (feed time = 30 min and T_j = 25 °C) of the product yield, heat accumulation profile and solution temperature.

Figure 2.3 represents the large scale scenario (V = 2500 L), where the feed time is 30 min, which corresponds to a dosing volumetric flow rate of 4.5 L/min. This scenario temperatures and heat profiles are presented throughout the reaction extension, represented by the product yield, in black. The reaction reaches 100% yield around 46 min based on the reactions kinetic model and the feed profile. Figure 2.3 highlights the solution temperature profile (in red) against the jacket temperature (imposed and equal to 25 °C, in blue). It is important to note the temperature profile, which in these conditions reaches a maximum point at the end of the feed (27.6 °C). For safety reasons, see Section 1.4, the reaction heat accumulation profile (%) was also calculated and it is represented in yellow: at the beginning of the reagent addition, the heat accumulation increases, reaching the maximum value (20%) around the end of the charging operation, at approximately 26 min.

As explained in Section 1.4, the heat accumulation is estimated through the different of the ideal heat and the real heat. The heat accumulation can create dangerous events, for instance if the reactor cooling system fails, so it should be maintained in low values.

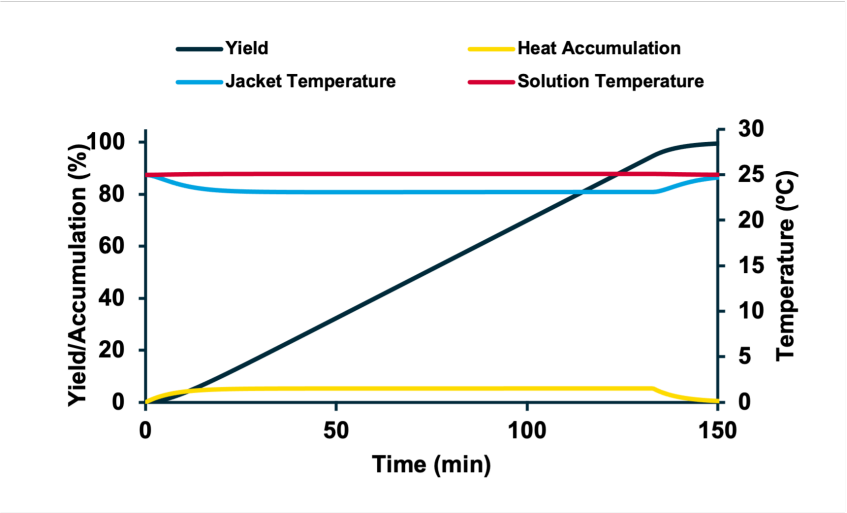

Figure 2.4: Optimized Heat accumulation scenario: scale up prediction (feed time = 2 h 13 min and T_j = 23 °C) of product yield and solution temperature.

Thus, Figure 2.4, results from an optimized scenario where the feed time and T_j were changed to minimize the maximum heat accumulation to 5% (a sufficient value for the temperature to be constant). The results show a dosing controlled reaction (see Section 1.4): feed time equals to 2 h and 13 min. Hence, the safety of the scale up operation is assured if the feed time is around 2 h and decreasing T_j during the feed time. If the cooling system fails, for instance, the addition could be paused, stopping the releasing energy under the form of heat.

As explained in Chapter 1, a good optimization results in a set of conditions in which quality and safety are assured. This is an example of a reaction optimization performed without any production data, demonstrating the powerful outcomes of kinetic and thermodynamic modelling. Many other simulations could be presented in this section, according to one's needs. For instance, if there is another parameter easily manipulated, the optimization could be done by changing that variable. Or if one needs to optimize reactants concentrations or reaction time, instead of heat accumulation.

It is worth highlighting that only 3 runs of the reaction were used to achieve the previous objectives, without taking samples. Therefore, the present work met its final goals: to evaluate what is the useful data for a descriptive kinetic and thermodynamic understanding of the reaction, to demonstrate the final aim of the methodology and its application.

3

Materials and Methods

Contents

When studying pharmaceutical reaction systems, both kinetic model proposal and corresponding parameter estimation can be challenging tasks. Having in mind a possible methodology to expedite this process, it is required to evaluate what would be the necessary lab procedure to determine a reaction mechanism and its parameters.
One of the most fast-forward approaches to this issue relies in stemming from a known chemical mechanism. For that, one may choose a widely studied reaction, for example the one described in chapter (*vide* Chapter 2), or one may use simulated data corresponding to a well defined system.
Therefore, the present chapter intends to describe the data generator used in this work. The generator describes a two step in series reaction, taking place in a lab reactor, in fed batch mode. The simulated experiments will be presented. Furthermore, in this chapter the models used for the modelling experiments will be described. Afterwards, the concentration and reaction heat data generated will be used as a replication of lab experiments for the systematic study – see Chapter 4 – simulating the output on-line or off-line analytical techniques and a reaction calorimeter.

3.1 Data Generator

The present data generator was developed using Microsoft® Office Excel ® and it was applied to generate concentration and heat flow data profiles.

The system simulated in this study comprises a fed-batch, lab-scale reaction calorimeter, with volume V, where it is conducted an homogeneous reaction, in isothermal mode. The reactant A is fed to the reactor, during a determined time (*feed time*), starting at the moment labeled *start of feed*.

The reaction taking place in the calorimeter is described by a two step mechanism. The generic reaction system represents any series mechanism composed by two steps of first-order kinetics Equation (3.1), where the corrected kinetic constants, k_1 and k_2, are described by a modified Arrhenius equation, eq. (3.2).

$$\mathrm{A} \xrightarrow{\mathrm{k_1}} \mathrm{B} \xrightarrow{\mathrm{k_2}} \mathrm{C} \tag{3.1}$$

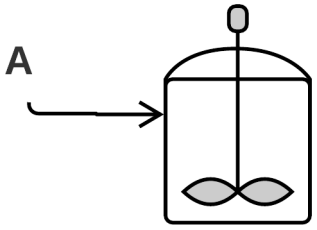

Figure 3.1: Schematic representation of the simulated system: semi-continuous reaction calorimeter.

$$k\left(T_r\right) = k\left(T_{ref}\right) \exp\left\{-\frac{E_A}{R}\left(\frac{1}{T_r} - \frac{1}{T_{ref}}\right)\right\} \tag{3.2}$$

Where T_r and T_{ref} represent the reactor temperature and the reference temperature respectively (K); $k(T_r)$ and $k(T_{ref})$ are the kinetic constants correspondent to each of the temperatures (min^{-1}); R represents the gas constant (kJ mol^{-1} K^{-1}) and E_a is the activated energy, kJ mol^{-1}.

Therefore, the rate law of each step (r_1, r_2) in mol min^{-1} is defined by eqs. (3.3) and (3.4).

$$r_1(t) = -k_1\, C_A(t)\, V \tag{3.3}$$

$$r_2(t) = -k_2\, C_B(t)\, V \tag{3.4}$$

Once the mechanism was described, it was possible to write the mass balances of the three generic components – eqs. (3.5) to (3.7).

$$V\frac{dC_A(t)}{dt} = C_A^{in} Q_v - r_1(t) \tag{3.5}$$

$$V\frac{dC_B(t)}{dt} = r_1(t) - r_2(t) \tag{3.6}$$

$$V\frac{dC_C(t)}{dt} = r_2(t) \tag{3.7}$$

Where V is the solution volume (mL), C_A, C_B, C_C are A, B, and C molar concentrations (mol mL^{-1}) and Qv is the feed flow-rate (mL min^{-1}). The mass balance equations allow the generation of the concentration profiles with time. On another hand, the heat released (positive) or consumed (negative) by the reaction ($\dot{q}_r$) can be calculated by the eq. (3.8).

$$\dot{q} = \dot{q}_r = -\sum(r_i \Delta H_{ri}) = -(r_1 \Delta H_{r1} + r_2 \Delta H_{r2}). \tag{3.8}$$

Note that the heat flow rate ($\dot{q}$, W) is equal to the reaction heat ($\dot{q}_r$, W). The heat flow rate is positive if the reaction is exothermic ($\Delta H_r < 0$) and vice-versa. To simplify the heat balance, the inlet stream was considered to be at the same temperature than the solution ($\dot{q}_{in} = 0$). Additionally, in these chemical system there is no phase change or tangible mixing phenomena. Also, this generator does not include stirring heat ($\dot{q}_{stirrer}$), dissipated heat ($\dot{q}_{loss}$) or the heat transferred by the calorimeter jacket ($\dot{q}_{flow}$). The heat associated to these inner components was considered to be negligible.

The differential equations were solved numerically, using Euler method.

Once the data was generated through the balance equations, *MS* Excel® *random* function was used in order to add noise to the generated data, replicating the noise associated to the lab measurements. For that, the random generated numbers uniformly distributed between 0 and 1 were transformed into a complex normal distribution $f(\mu, \sigma)$ with mean $\mu = 0$ and variance $\sigma^2 = 1$, by applying the following equation system, eq. (3.9).

$$\begin{aligned} z_1 &= \sqrt{-2 \ln x_1} \cos(2\pi x_2) \\ z_2 &= \sqrt{-2 \ln x_1} \sin(2\pi x_2) \end{aligned} \tag{3.9}$$

The result of this transformation represented by z_1 and z_2 was added to the data.

3.2 Reaction Parameters

Since the data generator math fundamentals are already described, the parameters simulated may be presented. The Table 3.1 summarizes the kinetic and thermodynamic parameters of the reaction (eq. (3.1)).

Table 3.1: Kinetic and thermodynamic parameters of each step of the reaction system.

Reaction Step i	k_i (Tref = 313.15 K) min^{-1}	Ea_i kJ mol^{-1}	ΔH_{ri} kJ mol^{-1}
1	0.2	80	-120
2	0.4	80	60

The reaction starts with a slow exothermic step, followed by a faster endothermic step. The reader may notice that the kinetic constants have the same order of magnitude, although step 2 is two times faster than step one ($\frac{k_2}{k_1} = 2$). On another hand, both steps have the same dependence of the temperature, expressed by identical Ea value.

3.3 Virtual experiments

Based on the Equation (3.1) reaction, several experiments were simulated not only by changing the temperature but also by varying the added noise. Note that further conditions were kept constant and they are discriminated in Table 3.2.

Table 3.2: Experiments description: common condition parameters.

Parameter	Unit	Value
V_0	mL	400
Q_v	mL min^{-1}	10
C_A^{in}	M	1
Feed time	min	2
Start of feed	min	1

Figure 3.2 presents the generator output of the experiments at 25°C. It demonstrates the difference on the generator output with the noise, replicating the data coming from a reaction calorimeter and for instance an on-line spectroscopic probe. Additionally, the experiment at 55 °C is presented in Figure 3.3 to illustrate the difference on the heat and concentration profiles with the temperature. This experiment is used in the double experiment study (see Section 4.2).
Furthermore, selecting discrete concentration points of the time profile, it was easily possible to generate virtual experiments replicating off-line sampling, alternatively to on-line (see Figure 3.4).

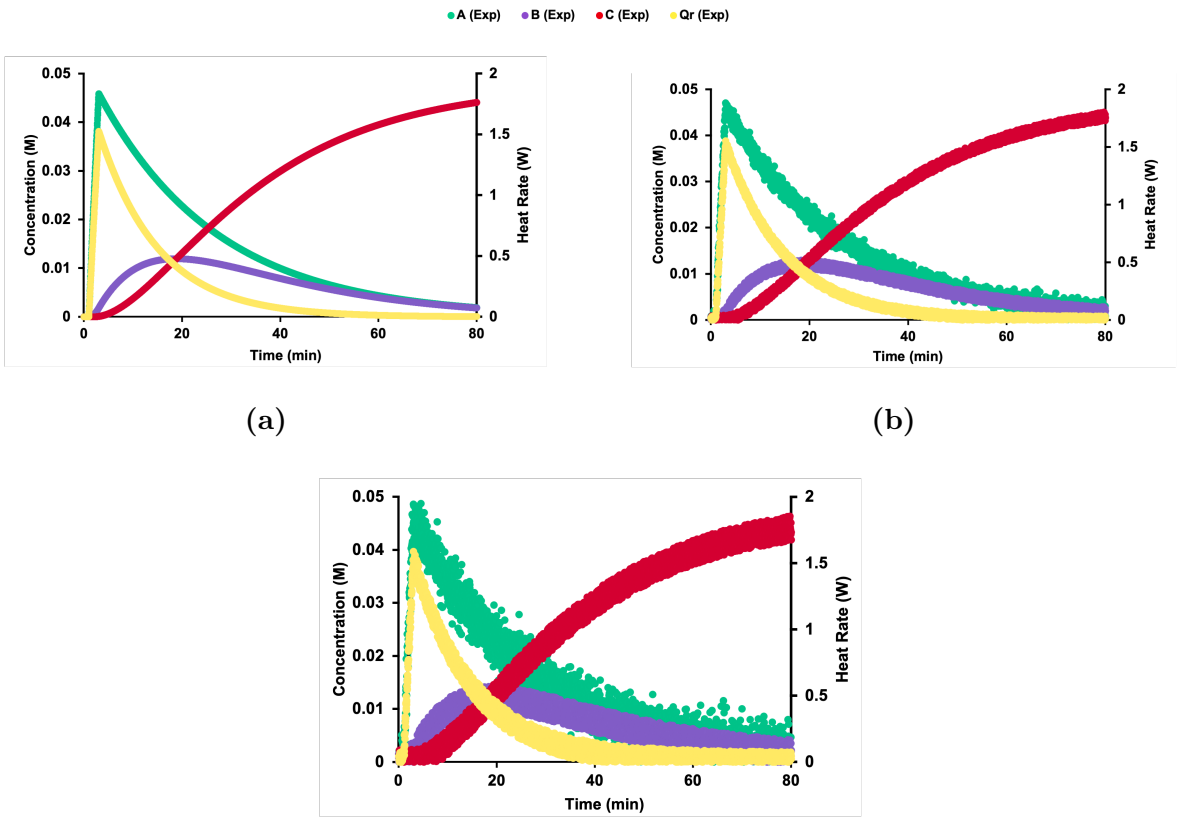

Figure 3.2: Generator output: concentration and heat profiles data at 25^{o}C with feed time of 2 min (a) σ=0.00 (b) σ=0.02 (c) σ=0.05.

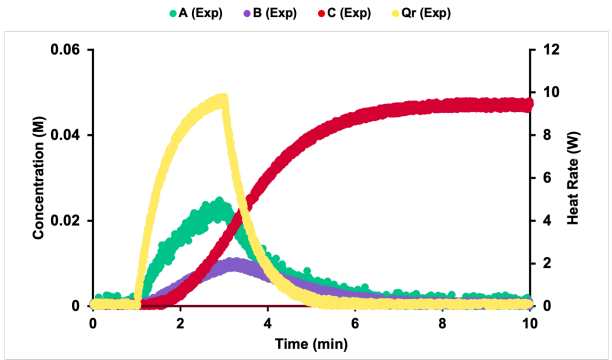

Figure 3.3: Generator output: concentration and heat profile data at 55 °C with feed time of 2 min (σ = 0.02).

The selection of the virtual samples was done in order to cover the reaction extension. For instance, at 25 °C, it was simulated the sampling at the following times, t = 0, 15, 30, 60, 80 min, covering the beginning of the reaction, the chemical transformation and the stationary state. Since the reaction becomes faster with temperature, at 55 °C, less samples were taken, although the rational was the same: t = 0, 2, 15, 27 min.

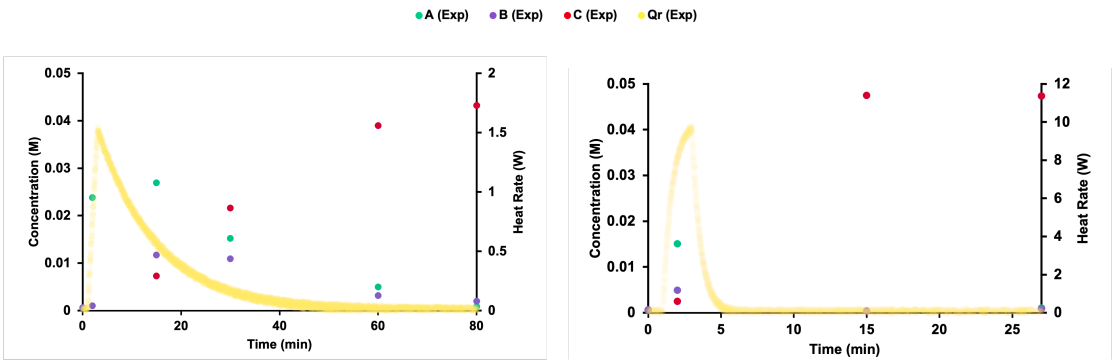

(a) **(b)**

Figure 3.4: Generator output: concentration samples and heat profile data at feed time of 2 min at (a) T=25°C (b) T=55°C.

3.4 *Excel* model

Once the simulated system data were generated, it was possible to calculate the k_1, k_2, Ea_1, Ea_2 H_{r1} and H_{r2} by the fitting the model to the experimental data. The Excel ® *solver* was implemented to minimize the sum of squares of the residues objective function, $f_{ob}^{(1)}$, see Equation (3.10).

$$f_{ob}^{(1)} = \sum (y_{exp}(t) - y_{model}(t))^2 \tag{3.10}$$

Where y may be the instant heat rate ($\dot{q}$).
On another hand, when it is intended to calculate the objective function with both heat rate and concentration data, the solver objective function $f_{ob}^{(2)}$ is used – Equation (3.11).

$$f_{ob}^{(2)} = \frac{\sum (y_{exp}(t) - y_{model}(t))^2}{\max(y(t))} \tag{3.11}$$

3.5 DynoChem® model

The program model uses the same kinetic. thermodynamic and math fundamentals. This model comprises *Rosenbrock* integration solver and a *Levenberg Marquardt* fitting solver.

4

Systematic Study

Contents

This chapter reports the results of the systematic study, using the data previously generated (*vide* Chapter 3) and its discussion. The referred data was used to test both models: the one built during this work (*Excel*® model) and the one using Dynochem®, from now on referred to as DC model.
The results are divided in two main sections. The first being the study using a single experiment (see Section 4.1), followed by the two-experiment research results (see Section 4.2).

It is worth noting that for all the modelling experiments, whether using the *Excel* model or DC, the solver was run two times in order to avoid any misleading results derived from local minimum values.

4.1 Single experiment results

The first approach was based on a single experiment, at 25 °C (Figure 3.2). Using this experiment, it was possible to estimate k_i and ΔHr_i. However, since it is not possible to determine Ea_i value with one single isotherm experiment, this value was kept out of the iterative calculation (and equal to the reference one, 80 kJ mol^{-1}). Each data set, whether it was heat rate or concentration data, comprises 3021 points, which corresponds to $\Delta t = 0.025$ min.

The systematic study scheme was based in performing several modelling experiments using only calorimetry data, as well as using heat combined with concentration data, according to the initial value (initial iterative number). The systematization of the initial iteration values allows the direct comparison of the different results. By testing different initial iterative numbers, one can identify what is the working range of the model. Furthermore, it allows the assessment of the effect of detection error, or noise, in the results.

Therefore, standardized initial values were tested, with different deviation from the reference parameters: 10%, 50%, 100%. Additionally, generic initial values were tested, which have no relation with the correct values or between themselves. The initial iterative numbers tested against the correct values are presented in Table 4.1 (note the deviation from the correct values when applicable).

Table 4.1: Systematic study arrangement: reference values against the initial iteration values tested on the single experiment study.

Parameter	Value	Initial Iteration Number				
		I	II	III	IV	V
k_1 (min^{-1})	**0.0416**	0.0454	0.0619	0.0825	0.1	0.01
k_2 (min^{-1})	**0.0825**	0.0908	0.124	0.165	0.1	0.01
ΔH_{r1} (kJ mol^{-1})	**-120**	-132	-180	-240	-120	-120
ΔH_{r2} (kJ mol^{-1})	**60**	66	90	120	-120	-120
Deviation		10%	50%	100%	-	-

The noise associated to the data was varied in order to assess its influence on the modelling results. Section 4.1.1 deals with the modelling results without added noise to the generated data, followed by the Section 4.1.2 where the experimental measurements were simulated with noise ($\sigma = 0.02$).

4.1.1 No noise

First of all, the *Excel* model performance was tested using no noise associated to the data, expressed by $\sigma = 0$. Starting from 10% deviation, corresponding to initial iteration number set I, the kinetic and thermodynamic parameters (k_1, k_2, ΔH_{r1} and ΔH_{r2}) were calculated. The first approach was the calculation of the parameters using calorimetry data only, see Figure 4.1.

The second approach was to calculate the same reaction parameters, using not only calorimetry data but also the concentration profiles, *vide* Figure 4.2.

Both these results are summarized in Table 4.2 along with the respective accuracy error values.

Table 4.2: Analytical results of the *Excel* model performance without noise associated to the data: stemming from 10% deviation values using calorimetry data with or without concentration data.

Parameter	Initial Iteration Number	Calorimetry		Calorimetry + Concentration	
		Result	Error (%)	Result	Error (%)
k_1 (min^{-1})	0.0454	0.0384	7.0	0.0413	0.0
k_2 (min^{-1})	0.0908	0.0825	0.0	0.0825	0.0
ΔH_{r1}(kJ mol^{-1})	-132	-129.0	7.5	-120.0	0.0
ΔH_{r2}(kJ mol^{-1})	66	69.0	15.1	60.0	0.0

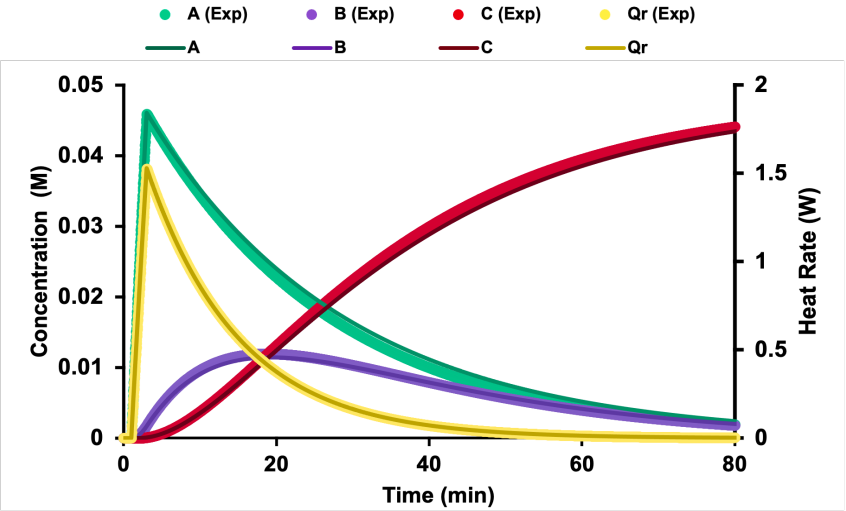

Figure 4.1: *Excel* model results (line) against experimental data (point) (T=25 °C, feed time =2 min), with no noise associated to the calorimetry data and stemming from 10% deviated initial iteration value.

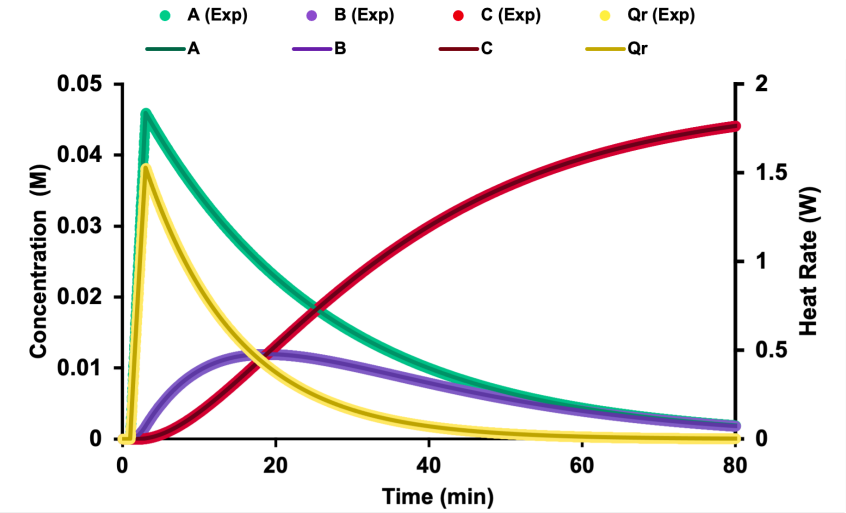

Figure 4.2: *Excel* model results (line) against experimental data (point) (T=25 °C, feed time =2 min) with no noise associated to the calorimetry data and stemming from 10% deviated initial iteration value.

From this first preliminary experiments, it can be concluded the model was capable of determining the kinetic and thermodynamic parameters, starting from 10% higher values from the reference. Figures 4.1 and 4.2 shows the model describing the experimental data. However, it is worth noting that even without added noise, using only calorimetry data, the results have an accuracy error associated (up to 15%). The use of the concentration profiles improves the results, expressed by approximately null error values (*vide* Table 4.2).

The same strategy was used to evaluate the DC model performance. Therefore, Figure 4.3 illustrates the outcome using only calorimetry data and Figure 4.4 represents the model results when adding A, B and C concentration profiles to the calorimetry data.

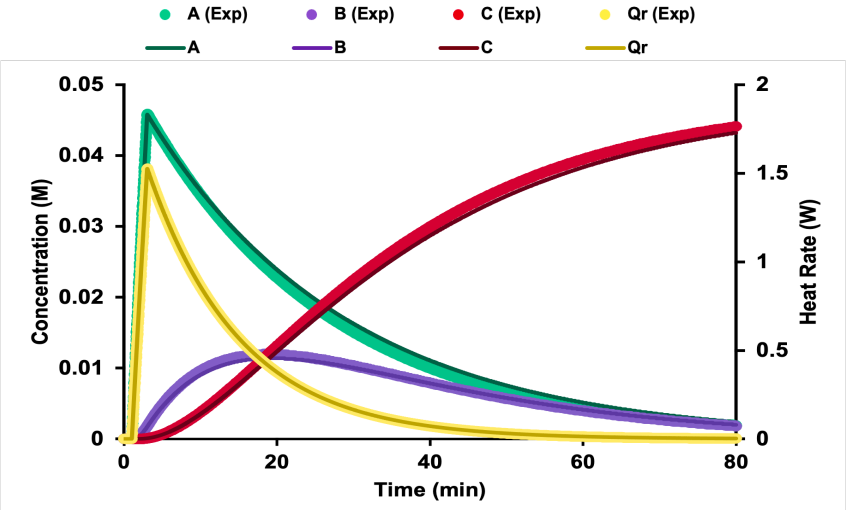

Figure 4.3: DC modelling results against the experimental data (T=25 °C, feed time = 2 min), with no noise associated to the calorimetry data and stemming from 10% deviated initial iteration value.

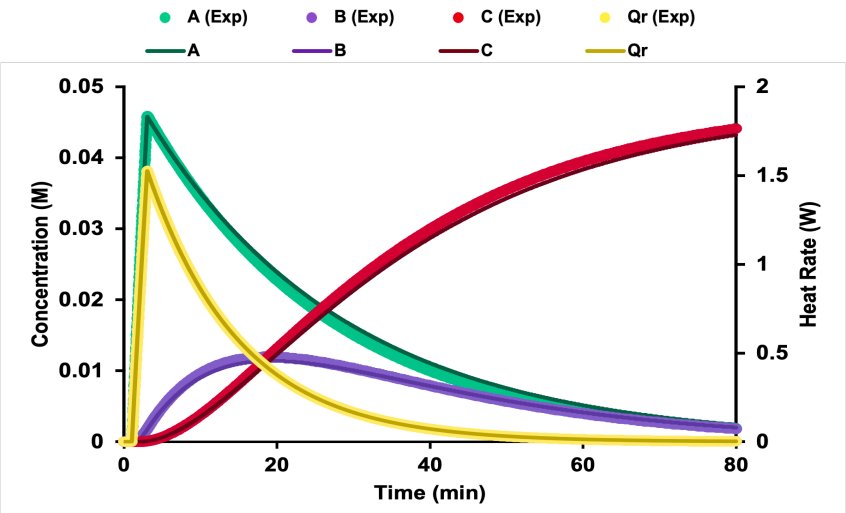

Figure 4.4: DC modelling results against the experimental data (T=25 °C), with no noise associated to the calorimetry and concentration data, and stemming from 10% deviated initial iteration value.

The results are once more summarized in the Table 4.3 along with the respective errors.

Table 4.3: Analytical results of the DC model performance without noise associated to the data: stemming from 10% deviation values using calorimetry data with or without concentration data.

Parameter	Initial Iteration Number	Calorimetry		Calorimetry + Concentration	
		Result	Error (%)	Result	Error (%)
k_1 (min^{-1})	0.0454	0.0384	6.9	0.0408	1.1
k_2 (min^{-1})	0.0908	0.0824	0.1	0.0822	0.4
ΔH_{r1}(kJ mol^{-1})	-132	-129.5	8.0	-125.8	4.8
ΔH_{r2}(kJ mol^{-1})	66	69.2	15.3	66.0	10.0

By analysing Table 4.3, it can be verified there is an improvement when adding the concentration profiles to the model, expressed by the smaller error values: 7% in opposition to 1% (k_1); 8% in opposition to 4% (ΔH_{r1}) and 15% in opposition to 10% (ΔH_{r2}). This is an expected result, which agrees with the conclusion taken from the similar experiment using the *Excel* model (vide Table 4.2). Comparing both Tables 4.2 and 4.3, it can be acknowledged an increase on the (accuracy) error values when using DC instead of the *Excel* model (results using concentration profiles). This shows a slightly better performance of the *Excel* model, when compared with DC.

After the previous experiments, the initial deviation was gradually increased, according to Table 4.1. The following results show the model response while stemming from 50% deviation values (II). Using the previous alignment, first it is presented the *Excel* model results using calorimetry data only (Figure 4.5), followed by the combined approach (Figure 4.6). Afterwards, the analytical results are presented in Table 4.4.

One can verify that when the reaction knowledge is limited (expressed by 50% margin from the correct values), the calorimetry data is not sufficient to achieve the correct concentration profiles, without readjusting the initial iterative value. There is no room from improvement on the fit of the calorimetry data (Figure 4.5), although the concentration profiles are not 100% accurate (Table 4.4).

By analysing both Table 4.2 and Table 4.4, one can verify a significant increase on the error values, specially when using only generated heat data. Therefore, when stemming from values further away from the reference ones the use of the concentration profiles becomes more significant.

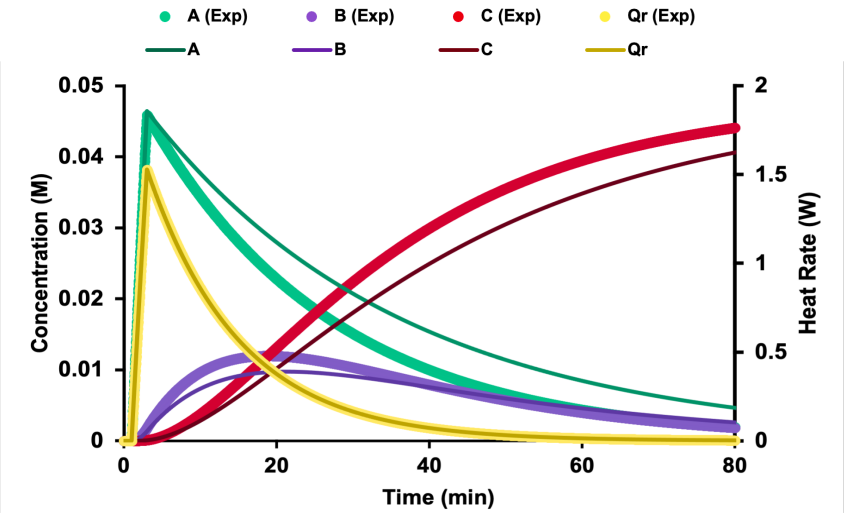

Figure 4.5: *Excel* model results (line) against experimental data (point) (T=25 °C, feed time = 2 min), with no noise associated to the calorimetry data and stemming from 50% deviated initial iteration value.

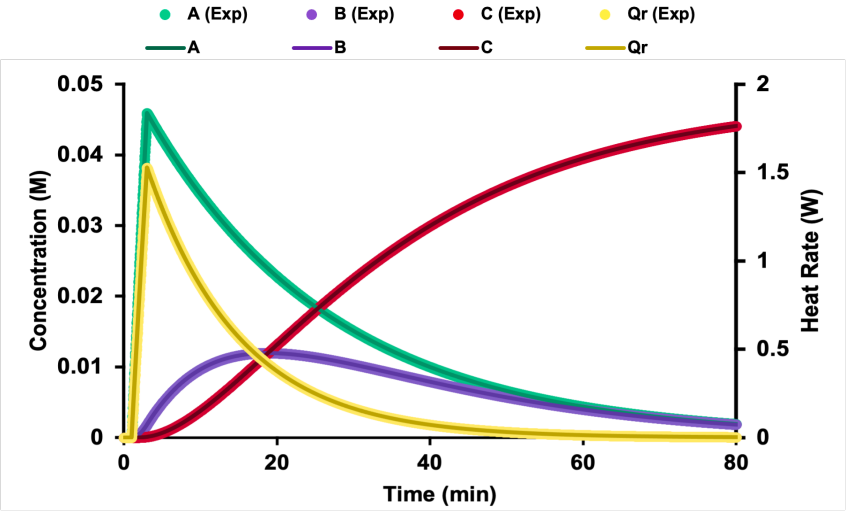

Figure 4.6: *Excel* model results (line) against experimental data (point) (T=25 °C, feed time = 2 min), with no noise associated to the calorimetry and concentration data, and stemming from 50% deviated initial iteration value.

The following figures result from the same modelling experiment yet using DC: parameter determination using calorimetry data only (Figure 4.7) and calorimetry data along with concentration data (Figure 4.8).
The analytical results are presented in Table 4.5.

Table 4.4: Analytical results of the *Excel* model performance without noise associated to the data: stemming from 50% deviation values using calorimetry data with or without concentration data.

Parameter	Initial Iteration Number	Calorimetry		Calorimetry + Concentration	
		Result	Error (%)	Result	Error (%)
k_1 (min^{-1})	0.0619	0.0299	27.5	0.0413	0.0
k_2 (min^{-1})	0.124	0.0825	0.0	0.0825	0.0
ΔH_{r1}(kJ mol^{-1})	-180	-165.6	38.0	-120.0	0.0
ΔH_{r2}(kJ mol^{-1})	90	105.6	75.9	60.0	0.0

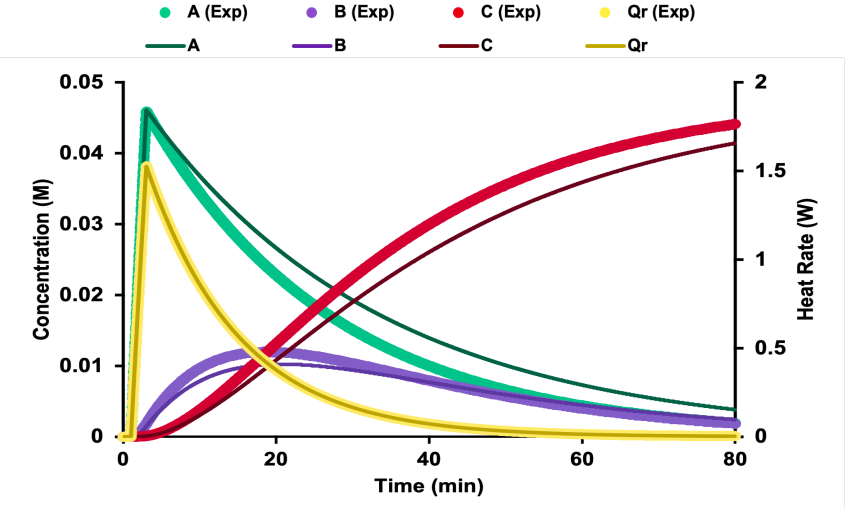

Figure 4.7: DC model results (line) against experimental data (point) (T=25 °C, feed time = 2 min), with no noise associated to the calorimetry data and stemming from 50% deviated initial iteration value.

Table 4.5: Analytical results of the DC model performance without noise associated to the data: stemming from 50% deviation values using calorimetry data with or without concentration data.

Parameter	Initial Iteration Number	Calorimetry		Calorimetry + Concentration	
		Result	Error (%)	Result	Error (%)
k_1 (min^{-1})	0.0619	0.0324	21.5	0.0408	1.1
k_2 (min^{-1})	0.124	0.0823	0.2	0.0821	0.5
ΔH_{r1}(kJ mol^{-1})	-180	-153.4	27.9	-125.5	4.6
ΔH_{r2}(kJ mol^{-1})	90	93.2	55.3	66.1	10.1

Once more, there is a significant improvement on the results when using the combined data. It is worth noting that, using the *Excel* model as well as using the DC model, the error associated to k_2 determination is approximately zero. Both models show better sensibility to the higher kinetic constant, corresponding to the second first order step.

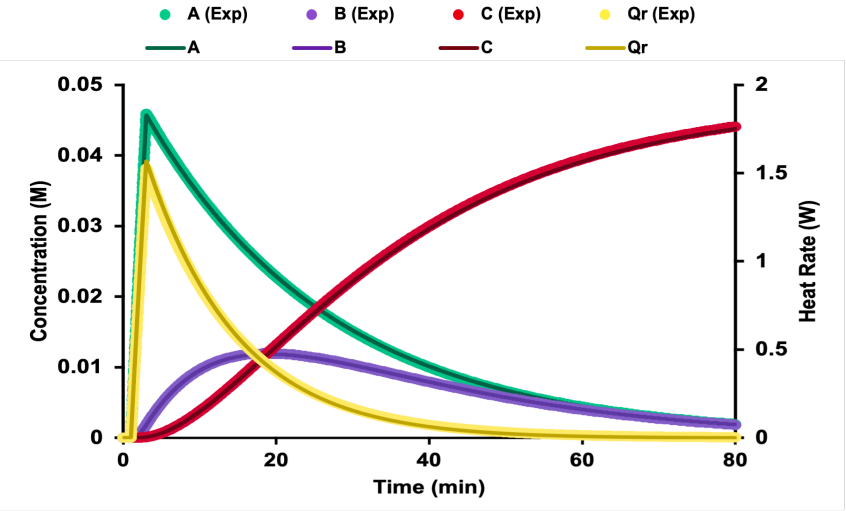

Figure 4.8: DC model results (line) against experimental data (point) (T=25 °C, feed time = 2 min), with no noise associated to the calorimetry and concentration data, and stemming from 50% deviated initial iteration value.

The results of modelling when starting from 100% deviated values are presented (III). These modelling experiments addressed the following issue: is the model capable of estimating the reaction parameters when stemming from 2 times higher corresponding values. The results of the *Excel* model are presented in Figures 4.9 and 4.10 followed by the DC outcomes Figures 4.11 and 4.12.Tables 4.6 and 4.7 summarize the *Excel* and the DC models corresponding analytical results.

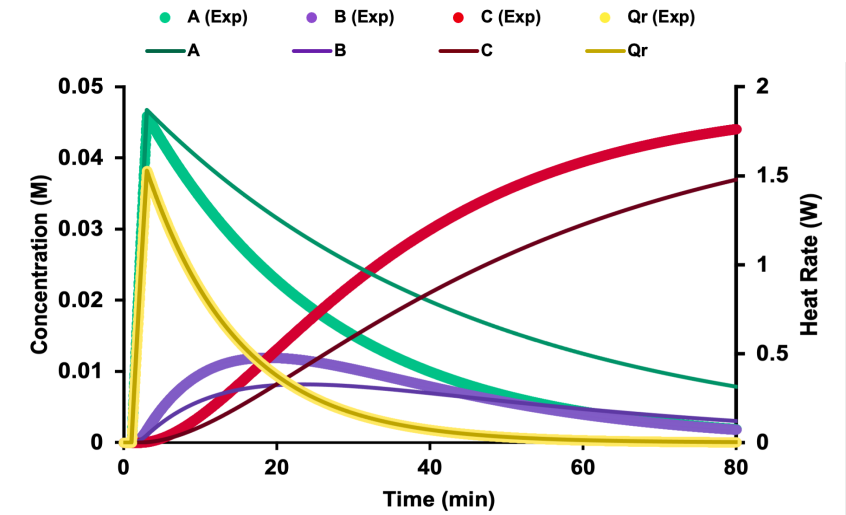

Figure 4.9: *Excel* model results (line) against experimental data (point) (T=25 °C, feed time = 2min), with no noise associated to the calorimetry data and stemming from 100% deviated initial iteration value.

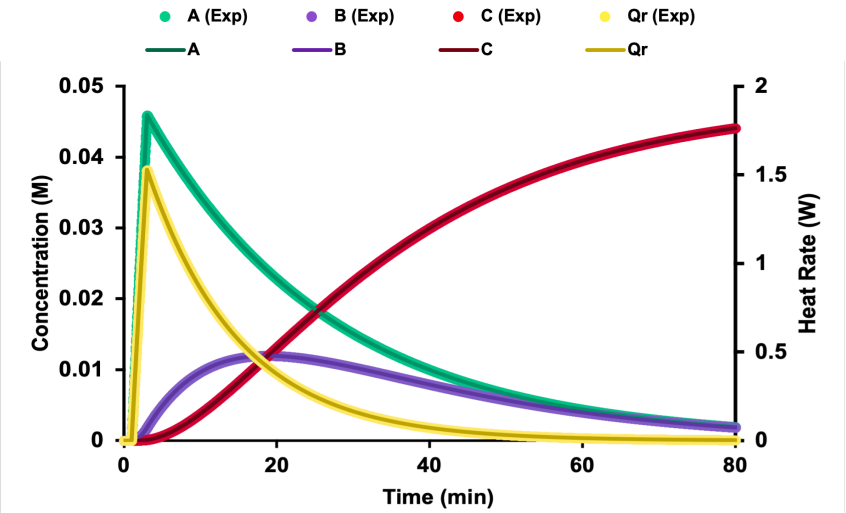

Figure 4.10: *Excel* model results (line) against experimental data (point) (T=25 °C), with no noise associated to the calorimetry and concentration data, and stemming from 100% deviated initial iteration value.

Table 4.6: Analytical results of the *Excel* model performance without noise associated to the data: stemming from 100% deviation values using calorimetry data with or without concentration data.

Parameter	Initial Iteration Number	Calorimetry		Calorimetry + Concentration	
		Result	Error (%)	Result	Error (%)
k_1 (min^{-1})	0.0825	0.0232	43.9	0.0413	0.0
textbfk_2 (min^{-1})	0.165	0.0825	0.0	0.0825	0.0
ΔH_{r1}(kJ mol^{-1})	-240	-213.7	78.1	-120.0	0.0
ΔH_{r2}(kJ mol^{-1})	120	153.7	156.2	60.0	0.0

Starting the iterative calculation from values two times larger than the reference, the results of the *Excel* model are congruous with the ones before. The heat profile is not sufficient to attain the correct parameters (Figure 4.9). As expected, when stemming from further values, the error associated to the parameters increases, according to Table 4.4 and to Table 4.6: 28 in opposition to 44%(k_1), 23 to 78% (ΔH_{r1}), 76 in opposition to 156% (ΔH_{r2}). Nevertheless, the addition of the three concentration profiles solves these limitations, as one can verify by the perfect fit (Figure 4.10) and approximately null error values (Table 4.6).

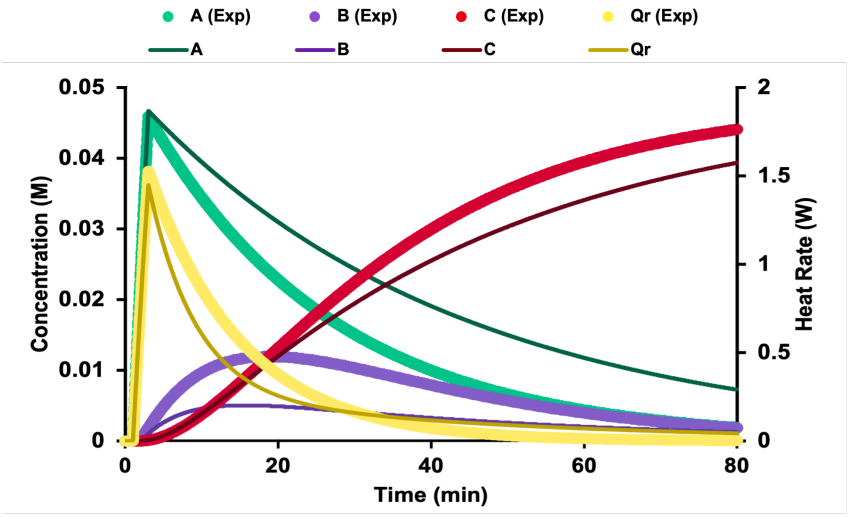

Figure 4.11: DC model results (line) against experimental data (point) (T=25 °C, feed time = 2 min), with no noise associated to the calorimetry data and stemming from 100% deviated initial iteration value.

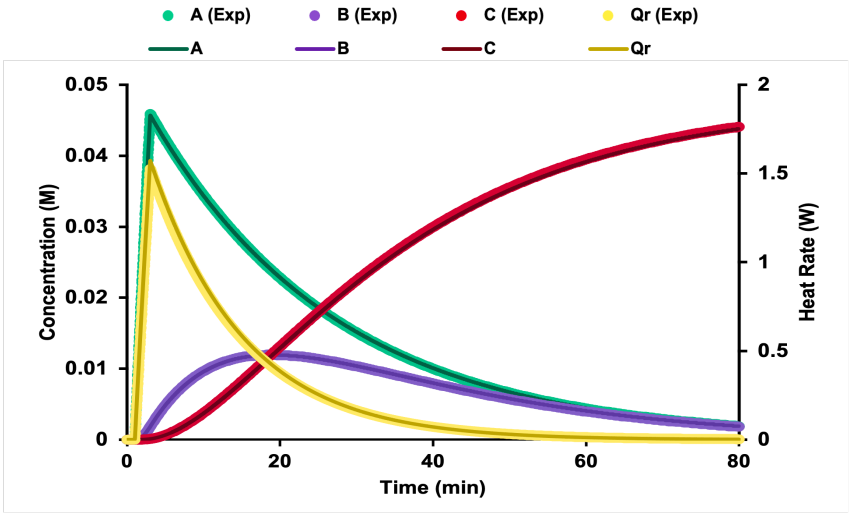

Figure 4.12: DC model results against experimental data (T=25 °C), with no noise associated to the calorimetry and concentration data, and stemming from 100% deviated initial iteration value.

Similar results were obtained when using the DC model, although this model was not able to attain the perfect heat profile fit, when using only calorimetry data (Figure 4.11). Despite, similar error values were associated to the analytical results from calorimetry data (Table 4.7). Regarding the outcomes of both calorimetry and concentration data, acceptable results were obtained (maximum error of 1% when using the *Excel* model, 6% when using the DC model).

Table 4.7: Analytical results of the DC model performance without noise associated to the data: stemming from 100% deviation values using calorimetry data with or without concentration data.

Parameter	Initial Iteration Number	Calorimetry		Calorimetry + Concentration	
		Result	Error (%)	Result	Error (%)
k_1 (min^{-1})	0.0825	0.0242	41.3	0.0409	0.8
k_2 (min^{-1})	0.165	0.0825	0.0	0.0815	1.2
ΔH_{r1}(kJ mol^{-1})	-240	-204.8	70.7	-125.2	4.3
ΔH_{r2}(kJ mol^{-1})	120	144.7	141.2	63.7	6.1

Following the sequential initial values tested (*vide* Table 4.1), generic values were tested: k_i=0.1 min^{-1} and ΔH_{ri} = -120 kJ mol^{-1}. This experiment is replicating a scenario where there is no manual fit to the data, neither any knowledge on the chemical behaviour of the components. Therefore, generic starting values were attempted. However, the *Excel* model was not capable of converging.

Thus, alternative generic values were tested: k_i=0.01 min^{-1} and ΔH_{ri} = -120 kJ mol^{-1} (Table 4.1). Once more, both model performances were assessed: Figures 4.13 and 4.14, Table 4.8 correspond to *Excel* model results and Figures 4.15 and 4.16, Table 4.9 present DC model results.

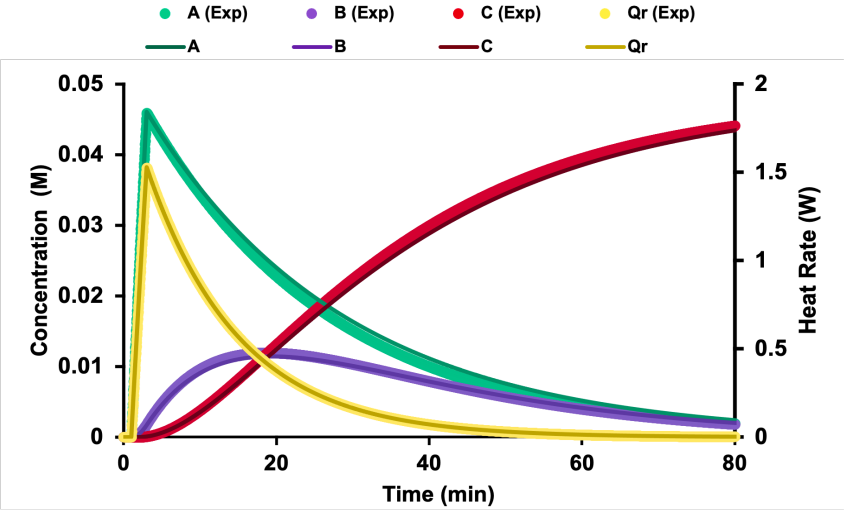

Figure 4.13: *Excel* model results (line) against experimental data (point) (T=25 °C, feed time = 2 min) with no noise associated to the calorimetry data and stemming from generic values.

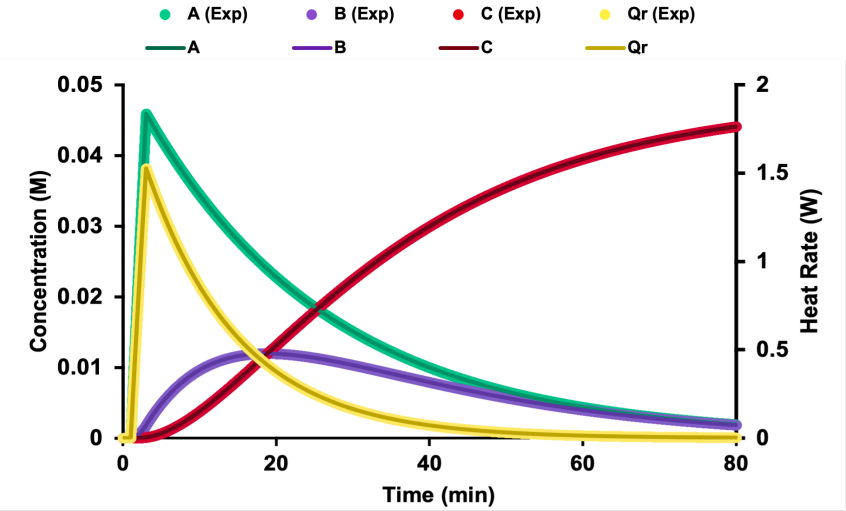

Figure 4.14: *Excel* model results (line) against experimental data (point) (T=25 °C, feed time = 2 min), with no noise associated to the calorimetry and concentration data, and stemming from generic values.

Table 4.8: Analytical results of the *Excel* model performance without noise associated to the data: stemming from generic values using calorimetry data with or without concentration data.

Parameter	Initial Iteration Number	Calorimetry		Calorimetry + Concentration	
		Result	Error (%)	Result	Error (%)
k_1 (min^{-1})	0.01	0.0825	100.0	0.0413	0.0
k_2 (min^{-1})	0.01	0.0	100.0	0.0825	0.0
ΔH_{r1}(kJ mol^{-1})	-120	-60.0	50.0	-120.0	0.0
ΔH_{r2}(kJ mol^{-1})	-120	-120.0	300.0	60.0	0.0

Table 4.9: Analytical results of the DC model performance without noise associated to the data: stemming from generic values using calorimetry data with or without concentration data.

Parameter	Initial Iteration Number	Calorimetry		Calorimetry + Concentration	
		Result	Error (%)	Result	Error (%)
k_1 (min^{-1})	0.01	0.0826	100.2	0.0409	0.8
k_2 (min^{-1})	0.01	0.0	100.0	0.0815	1.2
ΔH_{r1}(kJ mol^{-1})	-120	-60.0	50.0	-124.1	3.4
ΔH_{r2}(kJ mol^{-1})	-120	-120.0	300.0	62.9	4.8

Similar results were obtain, whether using built or DC models. Using only calorimetry data, it was not possible to estimate the correct parameters, within acceptable accuracy. It is necessary to include concentration results (Tables 4.8 and 4.9). According to the Figures 4.13 and 4.15, the model heat profile outlines the experimental heat profile. Nevertheless, the analytical results are not accurate, producing error values up to 300% (Tables 4.8 and 4.9).

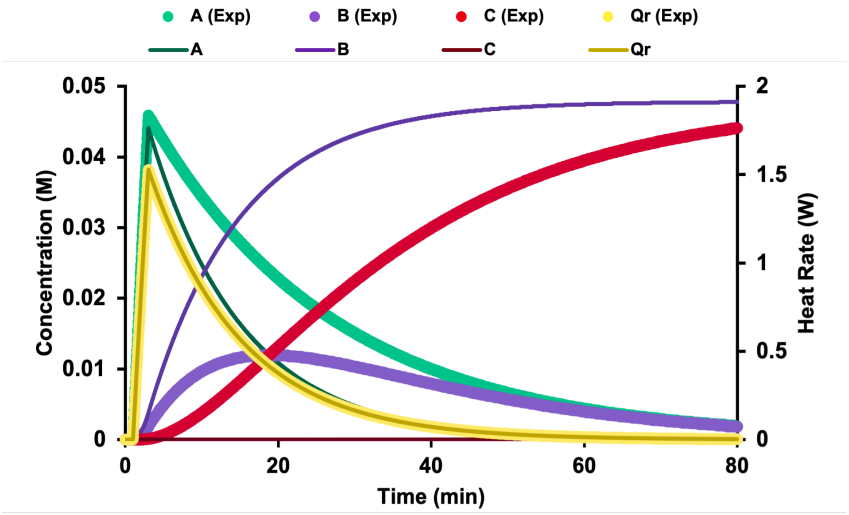

Figure 4.15: DC model results (line) against experimental data (point) (T=25 °C, feed time= 2min), with no noise associated to the calorimetry data and stemming from generic values.

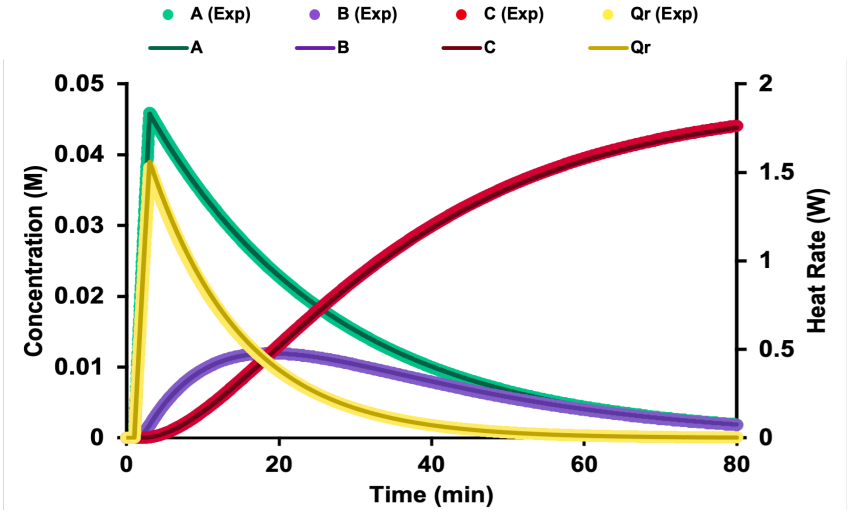

Figure 4.16: DC model results (line) against experimental data (point) (T=25 °C, feed time = 2 min), with no noise associated to the calorimetry and concentration data, and stemming from generic values.

Although it is not recommended to start the modelling without any manual fit to the data, in reality sometimes it happens. This experiment proves that it is not viable to rely on a calorimetry single experiment, nonetheless the model describes the system. In fact, one should always pre-fitting the data based on the chemical behaviour of the species at hand.

Overall, it was concluded that concentration data is crucial to have a descriptive knowledge of kinetic and thermodynamics of the consecutive 2-step chemical reaction. Furthermore, it is recommended to analyse the chemical system without rushing into the modelling experiments.

4.1.2 Moderate noise

Since the models were already tested without experimental noise associated to the data Figure 3.2(a), the modelling experiments using noise may be presented. The purpose of adding the noise to the data was to simulate the experimental outcome of a reaction calorimeter and on-line analytical techniques. In this section, it is presented the same modelling experiments, yet using the noise function on, when the data was generated: T=25^{o}C, feed time=2min, $\sigma = 0.02$ – Figure 3.2(b).

Following the same outline than before, the *Excel* model outcome, when the initial iterative numbers were 10% higher than the reference (I), are being presented. Figure 4.17 represents the model prediction against the experimental data, using only calorimetry data. On another hand, Figure 4.18 represents the modelling results using combined heat rate and concentration data.

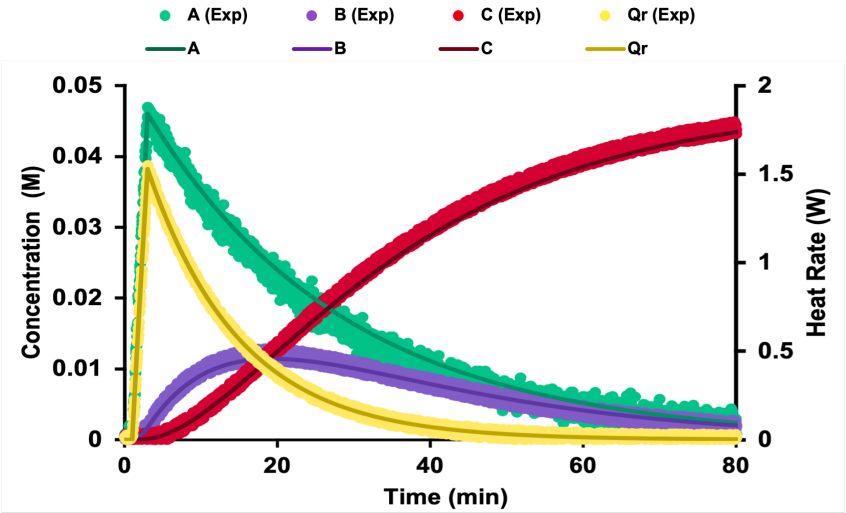

Figure 4.17: *Excel* model results (line) against experimental data (point) (T=25 °C, feed time = 2 min), stemming from 10% deviated initial iteration values, using calorimetry data with noise associated ($\sigma = 0.02$).

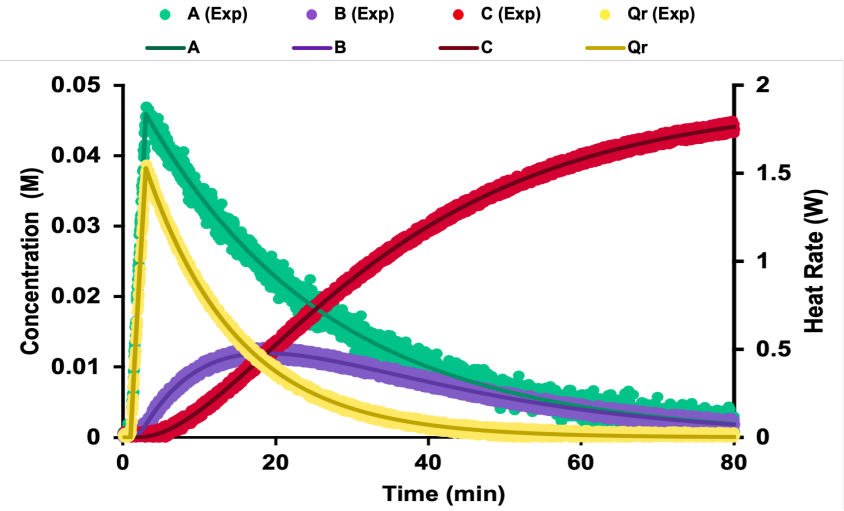

Figure 4.18: *Excel* model results (line) against experimental data (point) (T=25 °C, feed time = 2 min) and stemming from 10% deviated initial iteration values, using calorimetry and concentration data with noise associated ($\sigma = 0.02$).

According to the Figures 4.17 and 4.18, both model experiments are able to represent the data. From these figures, the noise does not interfere with the modelling results, starting from 10% deviated initial iterative numbers.
The analytical results are presented in Table 4.10.

Table 4.10: Analytical results of the *Excel* model performance: stemming from 10% deviation values, using calorimetry data with or without concentration data with noise associated ($\sigma = 0.02$).

Parameter	Initial Iteration Number	Calorimetry		Calorimetry + Concentration	
		Result	Error (%)	Result	Error (%)
k_1 (min^{-1})	0.454	0.0384	6.9	0.0412	0.0
k_2 (min^{-1})	0.908	0.0827	0.2	0.0826	0.2
ΔH_{r1}(kJ mol^{-1})	-132	-129.0	7.5	-120.1	0.1
ΔH_{r2}(kJ mol^{-1})	66	69.0	15.1	60.2	0.3

As expected, there is an improvement on the results, when concentration data was added, although the calorimetry data was sufficient to get a good result (stemming from 10% deviation).

The outcome of the calorimetry modelling experiment using DC model is represented in Figure 4.19, followed by the experiment using concentration Figure 4.20.

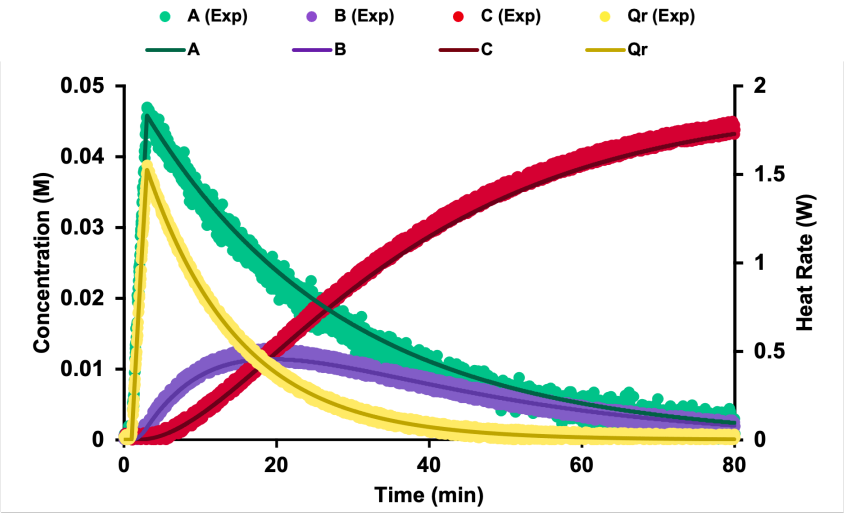

Figure 4.19: DC model results (line) against experimental data (point) (T=25 °C, feed time = 2 min), stemming from 10% deviated initial iteration values, using calorimetry data with noise associated ($\sigma = 0.02$).

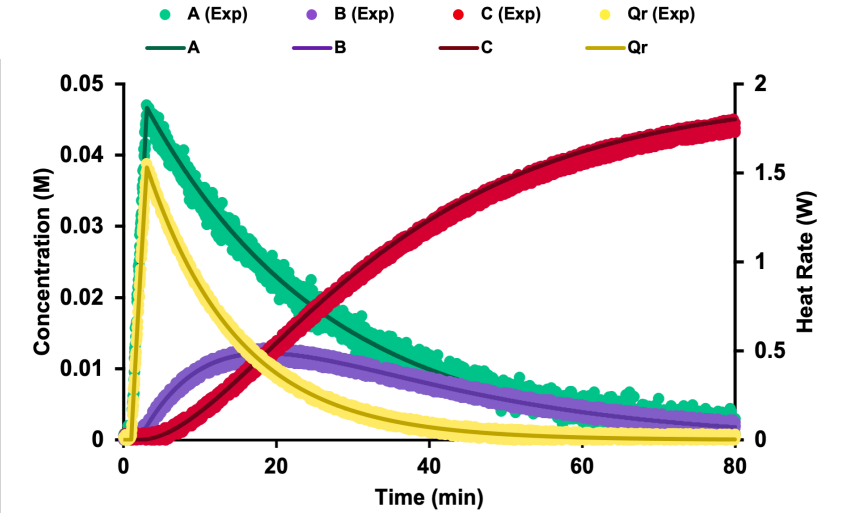

Figure 4.20: DC model results (line) against experimental data (point) (T=25 °C, feed time = 2 min), stemming from 10% initial iteration values, using calorimetry and concentration data with noise associated ($\sigma = 0.02$).

According to Figures 4.17 and 4.19 and Figures 4.18 and 4.20 there is no significant difference on the modelling results using the built or the DC model. The DC analytical results are presented in Table 4.11.

Table 4.11: Analytical results of the DC model performance: stemming from 10% deviation values, using calorimetry data with or without concentration data with noise associated ($\sigma = 0.02$).

Parameter	Initial Iteration Number	Calorimetry		Calorimetry + Concentration	
		Result	Error (%)	Result	Error (%)
k_1 (min^{-1})	0.0454	0.0384	6.9	0.0419	1.6
k_2 (min^{-1})	0.908	0.0824	0.1	0.0838	1.6
ΔH_{r1}(kJ mol^{-1})	-132	-129.6	8.0	-116.4	3.0
ΔH_{r2}(kJ mol^{-1})	66	69.4	15.6	57.6	4.1

As predicted, similar results were obtained using the DC. Furthermore, both model results agree with the previous experiment (Figures 4.1 and 4.3) and show no difference caused by the added noise.

In due course, iterative numbers 50% higher than the reference were tested (II).

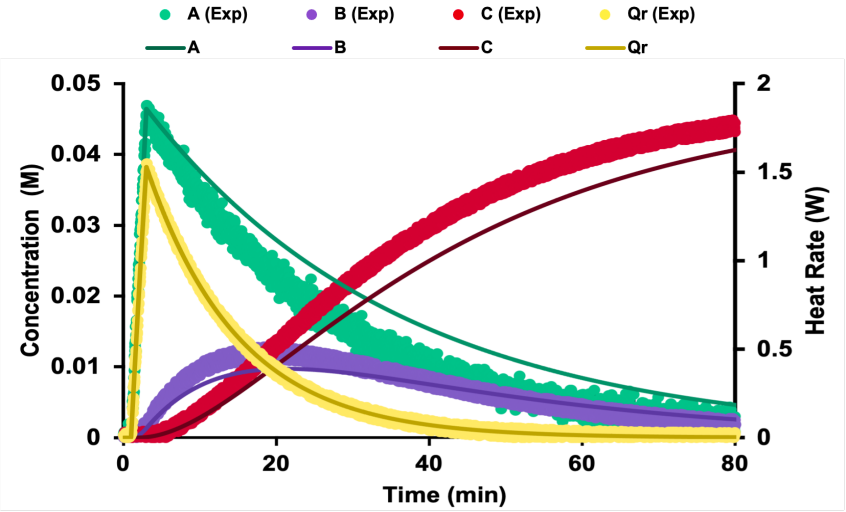

Figure 4.21: *Excel* model results (line) against experimental data (point) (T=25 °C, feed time = 2 min), stemming from 50% deviated initial iteration values, using calorimetry data with noise associated ($\sigma = 0.02$).

Regarding the *Excel* model performance using only calorimetry data (Figure 4.21): although the heat rate profile outlines the experimental data, the predicted concentration profiles were not accurate. However, the model can predict accurately all the parameters when concentration profiles were added to the iterative calculation, Figure 4.22.

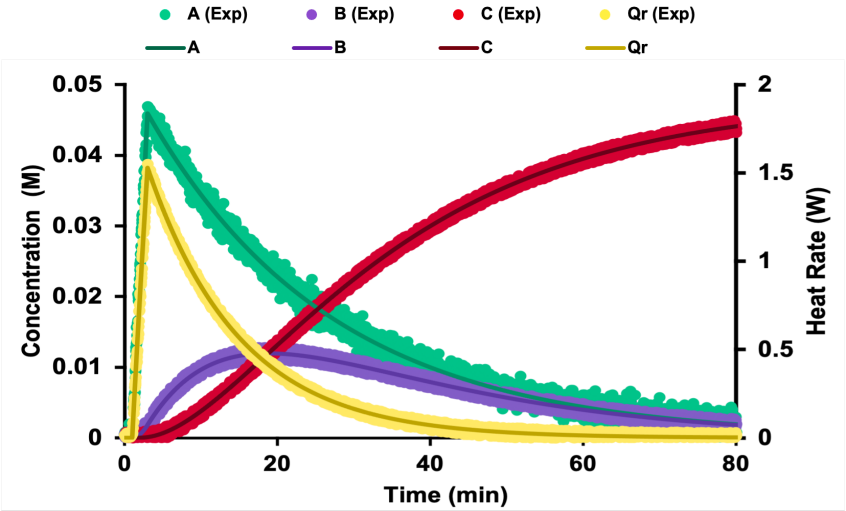

Figure 4.22: *Excel* model results (line) against experimental data (point) (T=25 °C, feed time = 2 min), stemming from 50% deviated initial iteration values, using calorimetry and concentration data with noise associated ($\sigma = 0.02$).

Table 4.12: Analytical results of the *Excel* model performance: stemming from 50% deviation values, using calorimetry data with or without concentration data with noise associated. ($\sigma = 0.02$).

Parameter	Initial Iteration Number	Calorimetry		Calorimetry + Concentration	
		Result	Error (%)	Result	Error (%)
k_1 (min^{-1})	0.0619	0.0299	27.5	0.0413	0.0
k_2 (min^{-1})	0.124	0.0827	0.2	0.0826	0.1
ΔH_{r1}(kJ mol^{-1})	-180	-165.5	37.9	-120.0	0.0
ΔH_{r2}(kJ mol^{-1})	90	105.6	76.0	60.1	0.2

The previous conclusion is supported by the Table 4.13. Comparing the results of this experiment with the experiment without noise (Tables 4.4 and 4.13), it is possible to conclude that the noise has no impact on the solution. In fact, the accuracy error values are exactly the same. Note these two modelling experiments were conducted with around 3000 points per data set. The results could be different if less points were used in the modelling experiment.

The DC outcome is shown in Figures 4.23 and 4.24.

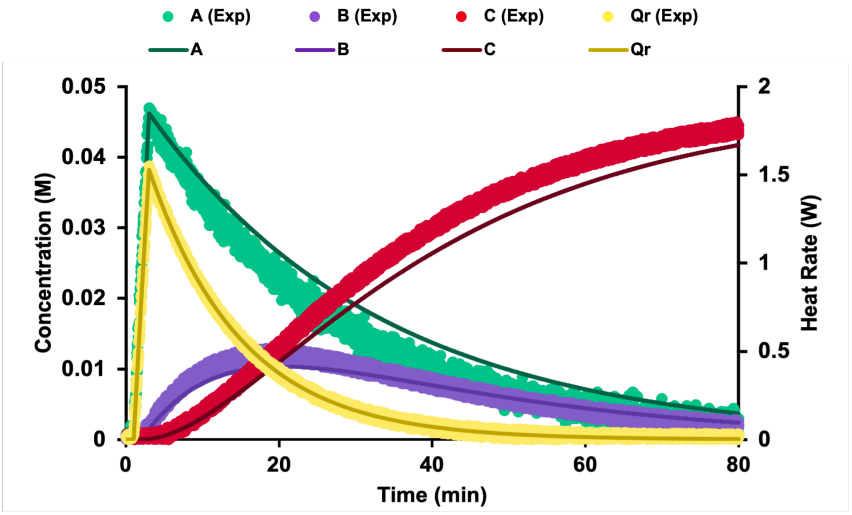

Figure 4.23: DC model results (line) against experimental data (point) (T=25 °C, feed time = 2 min), stemming from 50% deviated initial iteration values, using calorimetry data with noise associated ($\sigma = 0.02$).

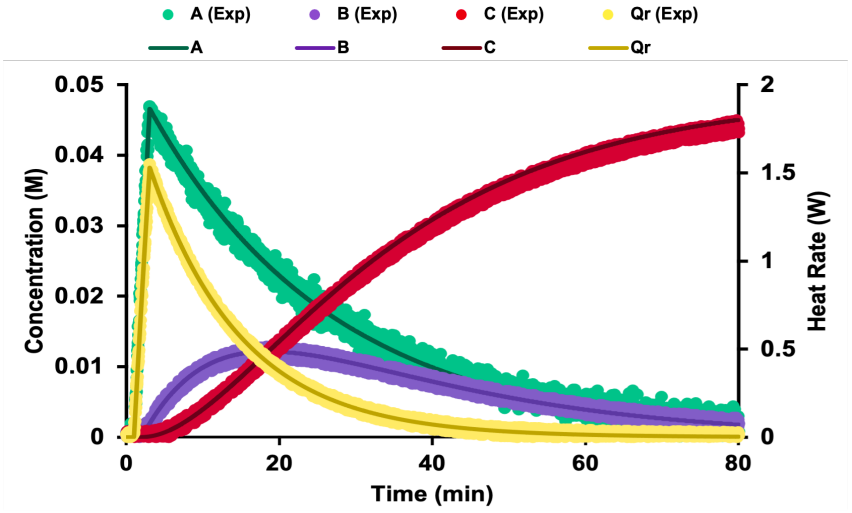

Figure 4.24: DC model results (line) against experimental data (point) (T=25 °C, feed time = 2 min), stemming from 50% deviated initial iteration values, using calorimetry and concentration data with noise associated ($\sigma = 0.02$).

DC model results show a slightly better performance (Figures 4.21 and 4.23), yet the results are commensurate with the previous ones (Table 4.15). Once more, the noise had no impact on the results (*vide* Tables 4.5 and 4.13).

Table 4.13: Analytical results of the DC model performance: stemming from 50% deviation values, using calorimetry data with or without concentration data with noise associated. ($\sigma = 0.02$).

Parameter	Initial Iteration Number	Calorimetry		Calorimetry + Concentration	
		Result	Error (%)	Result	Error (%)
k_1 (min^{-1})	0.0825	0.0329	20.2	0.0419	1.6
k_2 (min^{-1})	0.165	0.0827	0.2	0.0838	1.6
ΔH_{r1}(kJ mol^{-1})	-240	-151.0	25.8	-116.4	3.0
ΔH_{r2}(kJ mol^{-1})	120	91.0	51.6	67.6	4.1

Concerning the results when iterative initial numbers were twice as higher than the reference values (III), see Figure 4.25, the calorimetry data was not sufficient to describe the reaction system. This limitation was solved when the concentration was used on the modelling experiment – Figure 4.31.

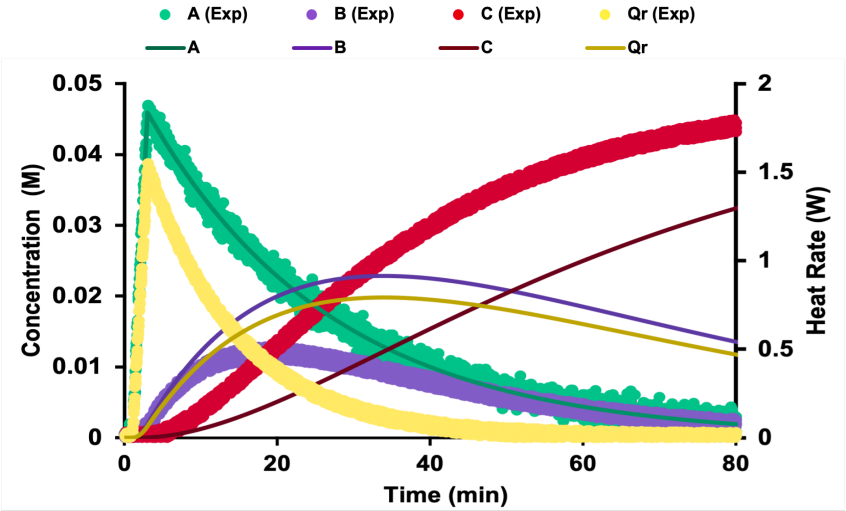

Figure 4.25: *Excel* model results (line) against experimental data (point) (T=25 °C, feed time = 2 min), stemming from 100% deviated initial iteration values, using calorimetry data with noise associated ($\sigma = 0.02$).

Table 4.14 analytical results show a better sensibility on the kinetic constants (error up to 43%) than the reaction heat values (error up to 158%). As predicted by the fit of the model to the experimental data in Figure 4.17.

The same experiment performed with DC model are presented below (Figures 4.27 and 4.28.

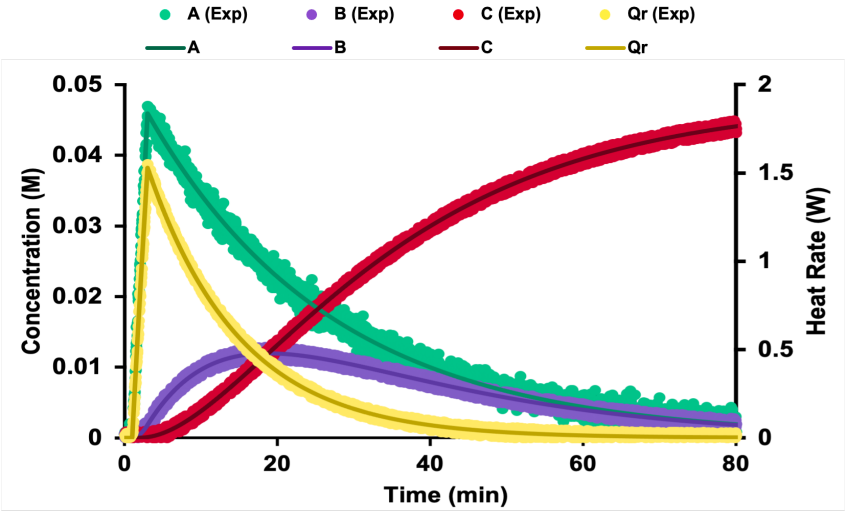

Figure 4.26: *Excel* model results (line) against experimental data (point) (T=25 °C, feed time = 2 min), stemming from 100% deviated initial iteration values, using calorimetry and concentration data with noise associated ($\sigma = 0.02$).

Table 4.14: Analytical results of the *Excel* model performance: stemming from 100% deviation values, using calorimetry data with or without concentration data with noise associated. ($\sigma = 0.02$).

Parameter	Initial Iteration Number	Calorimetry		Calorimetry + Concentration	
		Result	Error (%)	Result	Error (%)
k_1 (min^{-1})	0.0825	0.0232	43.8	0.0413	0.0
k_2 (min^{-1})	0.165	0.0827	0.2	0.0826	0.1
ΔH_{r1} (kJ mol^{-1})	-240	-213.7	78.1	-120.0	0.0
ΔH_{r2} (kJ mol^{-1})	120	153.8	156.3	60.1	0.2

According to Figure 4.27, through the fit of the heat profile the model was capable to predict a similar kinetic behaviour of the reaction, in a sense that the model concentration profiles have the same behaviour than the experimental one, in opposition to the *Excel* model results (Figure 4.25). Regarding the combined approach, the fitting of the four data sets results in a perfect fit, see Figure 4.28.

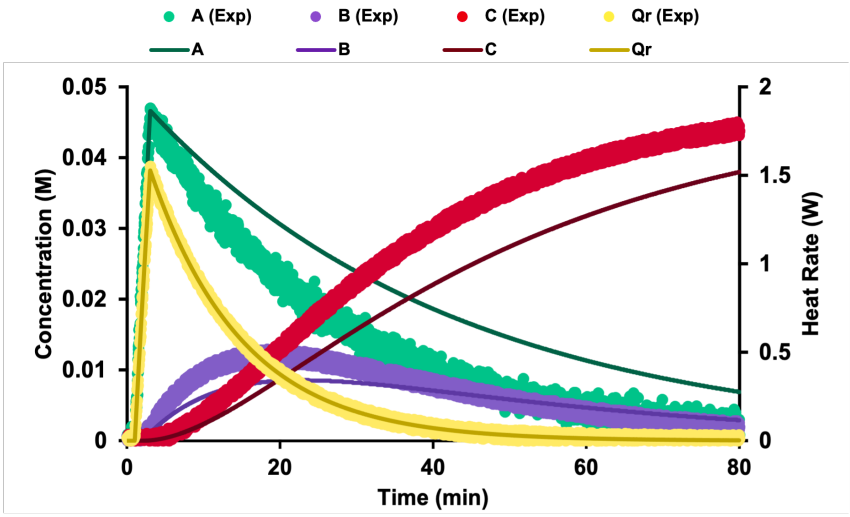

Figure 4.27: DC model results (line) against experimental data (point) (T=25 °C, feed time = 2 min), stemming from 100% deviated initial iteration values, using calorimetry data with noise associated ($\sigma = 0.02$).

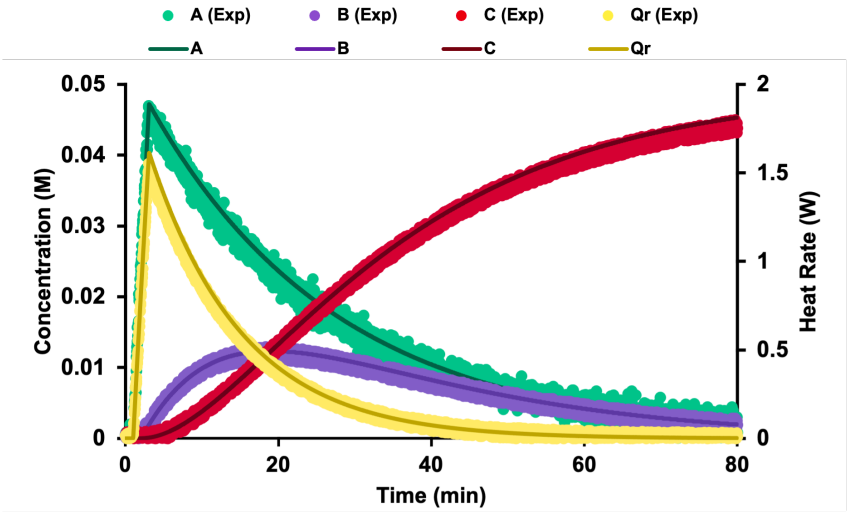

Figure 4.28: DC model results (line) against experimental data (point) (T=25 °C, feed time = 2 min), stemming from 100% deviated initial iteration values, using calorimetry data with noise associated ($\sigma = 0.02$).

Although, the concentration profile outcomes are close to the experimental profiles, when calorimetry data is being used to fit the model (Figure 4.27), kinetic and thermodynamic results obtained are not accurate (Table 4.15). In fact, there are error values associated to this experiment up to 141%. Nevertheless, these results were expected, since the analytical results using no noise associated to the data were the same Table 4.7. Once again, the noise had no impact on the model performance.

Table 4.15: Analytical results of DC model performance: stemming from 100% deviation values, using calorimetry data with or without concentration data with noise associated. ($\sigma = 0.02$).

Parameter	Initial Iteration Number	Calorimetry		Calorimetry + Concentration	
		Result	Error (%)	Result	Error (%)
k_1 (min^{-1})	0.0825	0.0248	39.9	0.0409	0.85
k_2 (min^{-1})	0.165	0.0827	0.3	0.0816	1.1
ΔH_{r1}(kJ mol^{-1})	-240	-199.8	66.5	-124.4	3.6
ΔH_{r2}(kJ mol^{-1})	120	139.9	133.1	63.1	5.2

At last, generic values were tested as initial iteration values: $k_1 = k_2 = 0.01$ and $\Delta H_{r1} = \Delta H_{r2} = -120$. The reader may notice, according to Table 4.1, IV initial values were not tested. This was a consequence of the previous experiment (without noise), since both models could not reach a good result.

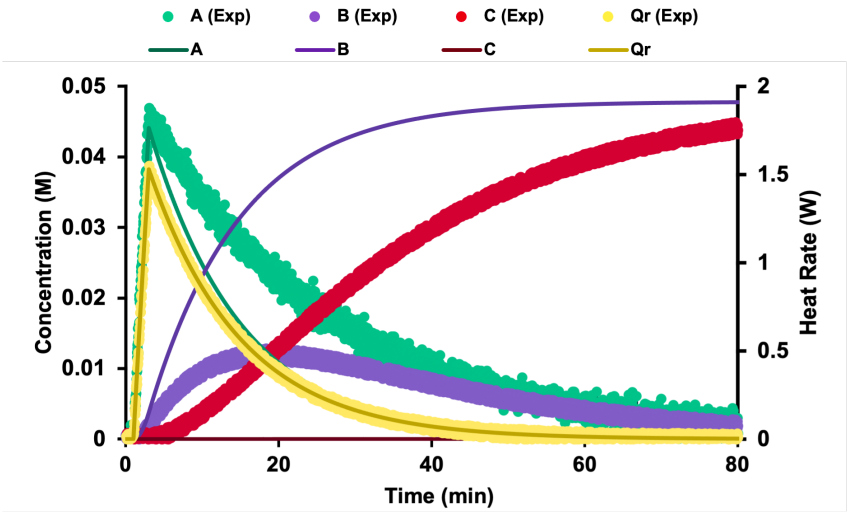

Figure 4.29: *Excel* model results (line) against experimental data (point) (T=25 °C, feed time = 2 min), stemming from generic initial iteration values, using calorimetry data with noise associated ($\sigma = 0.02$).

Figure 4.29 shows the outcome of the *Excel* model when fitting the model to the heat data. Considering this experiment, one can not predict all the reaction parameters, from one single experiment without foreknowledge on the kinetics. In fact, the model could not predict k_2, resulting in an overestimation of k_1 and of intermediate final concentration. Withal, concentration data combined with calorimetry data accomplished a good fit (Figure 4.29).

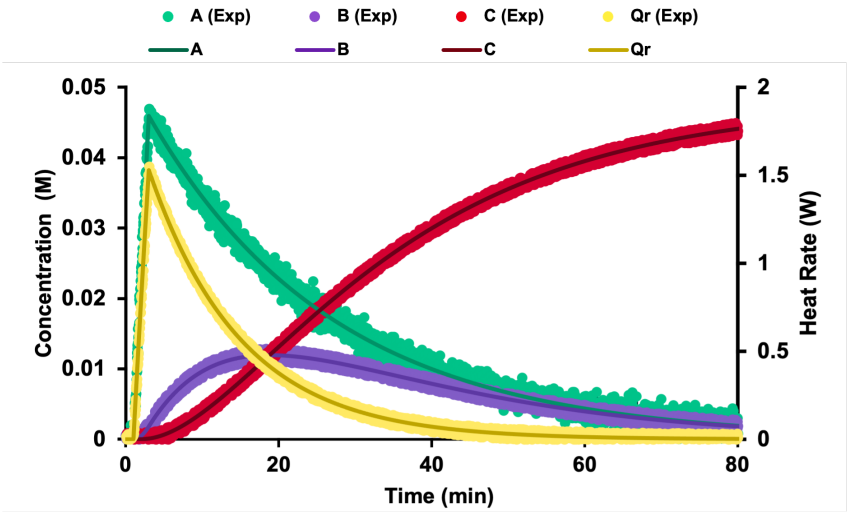

Figure 4.30: *Excel* model results (line) against experimental data (point) (T=25 °C, feed time = 2 min), stemming from generic initial iteration values, using calorimetry and concentration data with noise associated ($\sigma = 0.02$).

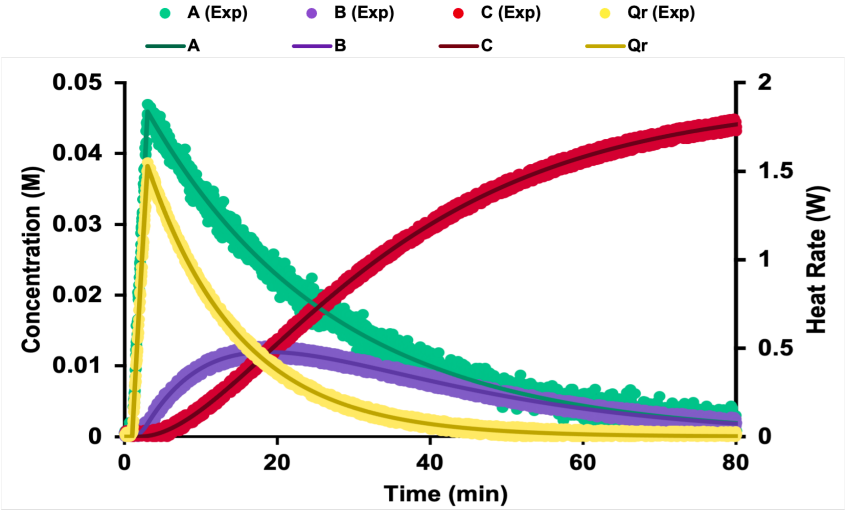

Figure 4.31: *Excel* model results (line) against experimental data (point) (T=25 °C, feed time = 2 min). 100% deviation between the starting values and the correct ones. Using calorimetry and concentration data with noise associated ($\sigma = 0.02$).

The reader may notice the significant error values (50-300%), when one single data set was used. Table 4.17 analytical results sustain not only the previous premise, but also the conclusion of the same experiment but without noise. One should always pre-fit the model to the data, having in mind the reaction kinetic behaviour, before modelling. The solution to this issue may be the addition of the concentration profiles, although this information is not always available. In fact, some components can not be identifiable through spectroscopic probes, for instance. Furthermore, intermediates can be particularly challenging to identify, if the mechanism is not known.

Table 4.16: Analytical results of the *Excel* model performance: stemming from generic values, using calorimetry data with or without concentration data with noise associated. ($\sigma = 0.02$).

Parameter	Initial Iteration Number	Calorimetry		Calorimetry + Concentration	
		Result	Error (%)	Result	Error (%)
k_1 (min^{-1})	0.01	0.0827	100.5	0.0413	0.0
k_2 (min^{-1})	0.01	7.57e-6	100.0	0.0826	0.1
ΔH_{r1}(kJ mol^{-1})	-120	-59.9	50.1	-120.0	0.0
ΔH_{r2}(kJ mol^{-1})	-120	-120.0	300.0	60.1	0.2

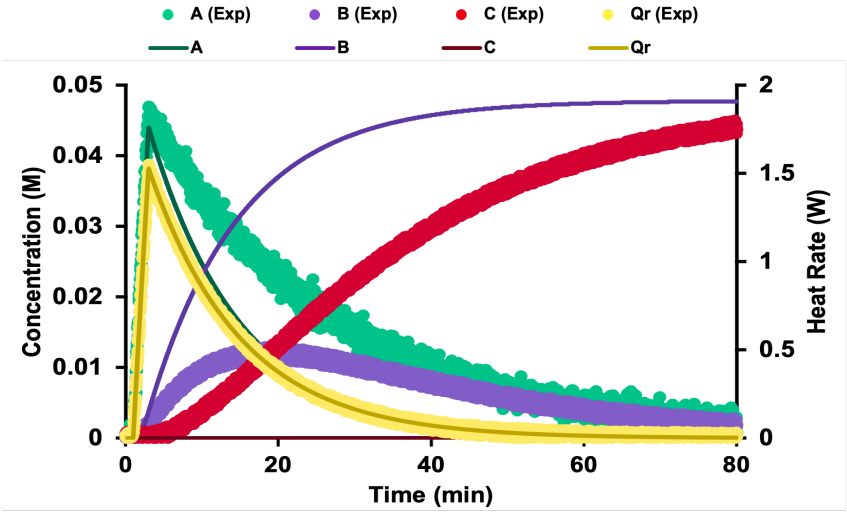

Figure 4.32: DC model results (line) against experimental data (point) (T=25 °C, feed time = 2 min), stemming from generic initial iteration values, using calorimetry data with noise associated ($\sigma = 0.02$).

Table 4.17: Analytical results of DC model performance: stemming from generic values, using calorimetry data with or without concentration data with noise associated. ($\sigma = 0.02$).

Parameter	Initial Iteration Number	Calorimetry		Calorimetry + Concentration	
		Result	Error (%)	Result	Error (%)
k_1 (min^{-1})	0.01	0.0828	100	0.0419	0
k_2 (min^{-1})	0.01	8.05×10^{-6}	100	0.0838	0
ΔH_{r1}(kJ mol^{-1})	-120	-60	50	-116	0
ΔH_{r2}(kJ mol^{-1})	-120	-120	300	60	0

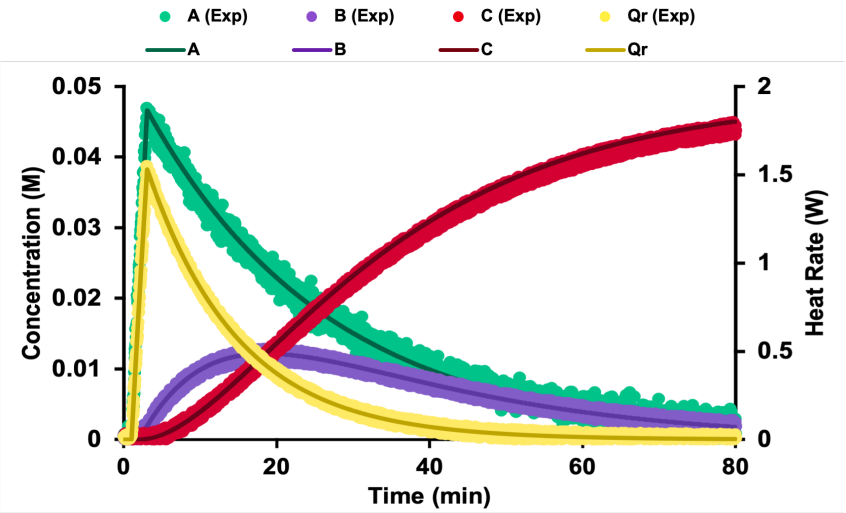

Figure 4.33: DC model results (line) against experimental data (point) (T=25 °C, feed time = 2 min), stemming from generic initial iteration values, using calorimetry and concentration data with noise associated ($\sigma = 0.02$).

Overall, the noise had no impact on the results. However, it is worth to highlight that these experiments were performed with a large number of points. The results could be different if less points were available. Sometimes, it is useful to reduce the number of points to optimize the modelling experiment or some species are not identifiable through spectroscopic probes. Furthermore, if spectroscopic probes were undertaken for limited samples (for example off-line HPLC samples) the experimental noise could get more significant.

Additionally, the model showed better sensibility to the kinetic constants than to the reaction enthalpy. Although, such result may be expected, according to the wider range of possible values, it should be taken into account while estimating these values – specially when only calorimetry data is used, to avoid misleading results on heat consumed or released. Besides, the heat rate characterization gets more significant when the reactor scale is increased (see Section 1.4).

Once more, the results using moderate noise associated do the heat and concentration profiles highlighted the importance of a combined strategy while estimating the kinetic and heat parameters of the reaction.

The results using elevated noise ($\sigma = 0.05$) are not presented in this work, since its magnitude was considered to be overestimated.

4.2 Double experiment results

In the present section, the modelling experiments presented were performed using data corresponding to two different runs of the same reaction, at two different temperatures. This approach is closer to the experimental reality as it allows the estimation of all kinetic parameters, including Ea_i. Therefore, the simulation includes two different isothermal essays (Figures 3.2(b) and 3.3.

For convenience reasons, all the modelling experiments were performed using the DC model, since the results of the previous study using DC were similar to the *Excel* model results. As in the previous study, the modelling experiments were conducted using calorimetry data only, as well as using calorimetry data along with concentration profiles. However, the following combined modelling experiments have only one concentration profile instead of three. It was chosen to use only one concentration profile, as it can be not possible to identify all the species involved in an actual reaction system. Thus, concentration of reagent A was used in those modelling experiments, replicating a situation where it would be the only species possible to identify.

In this section, experiments illustrated by Figures 3.2(b) and 3.3 were used to calculate all kinetic and thermodynamic parameters of the generic two steps reaction. These parameters were determined at $T_{ref} = 40$ °C. It is worth to highlight each data set of experiment at 25 °C comprises 3255 points ($\Delta t = 0.025$ min) and each data set of experiment at 55 °C had 5493 points (corresponding to $\Delta t = 0.005$ min).

As described previously, standardized initial iteration numbers were used to test the model performance, in order to straightly compare the different results. The correct parameter and the initial iteration numbers tested are summarized in Table 4.18.

Starting from 10% deviated initial iterative values, the results of modelling using calorimetry data only are represented in Figure 4.34, while the results using also A concentration profile are represented in Figure 4.35.

By analysing Figure 4.34, it is clear both of the experiments are described by the model, using only heat rate data. As expected, when a concentration profile is added, the model also outlines the experimental data, Figure 4.35.

Table 4.18: Systematic study arrangement: reference values against the initial iteration values tested on the double experiment study.

Parameter	Value	Initial Iteration Number				
		I	II	III	IV	V
k_1 (min^{-1})	0.2	0.22	0.1	0.02	1×10^{-4}	0.01
k_2 (min^{-1})	0.4	0.44	0.3	0.04	1×10^{-4}	0.01
Ea_1 (kJ mol^{-1})	80	72	40	8	60	60
Ea_1 (kJ mol^{-1})	80	72	40	8	60	60
ΔH_{r1} (kJ mol^{-1})	-120	-132	-60	-12	-120	-120
ΔH_{r2} (kJ mol^{-1})	60	66	30	-12	-120	-120
Deviation		10%	50%	90%	-	-

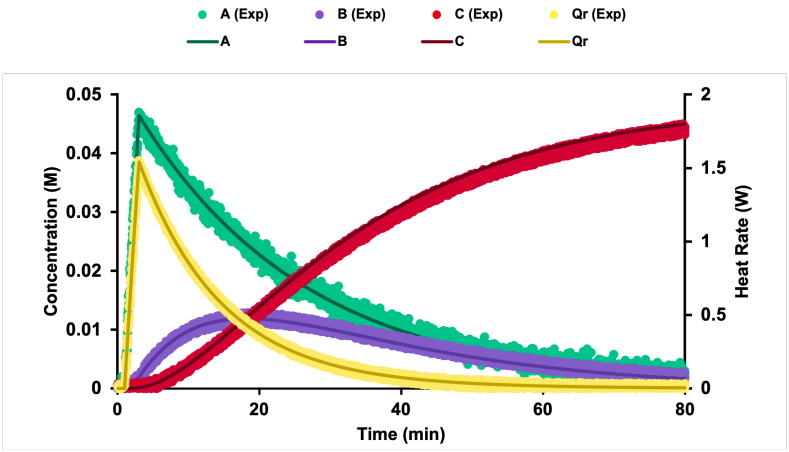

(a)

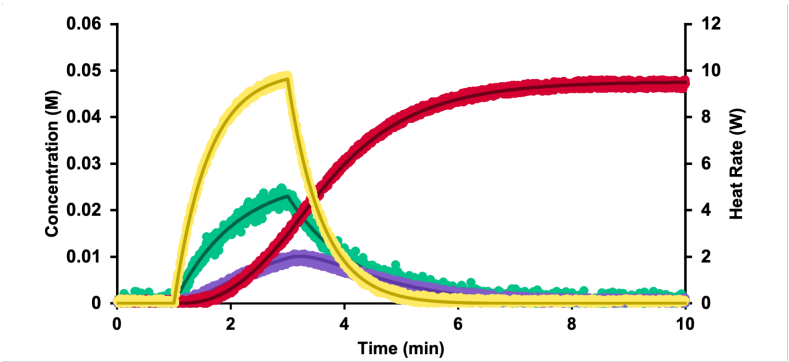

(b)

Figure 4.34: Modelling results with two experiments at two different temperatures (feed time = 2 min), stemming from 10% deviated initial iterative number, using calorimetry data ($\sigma = 0.02$) (a) at 25 ºC; (b) at 55 ºC.

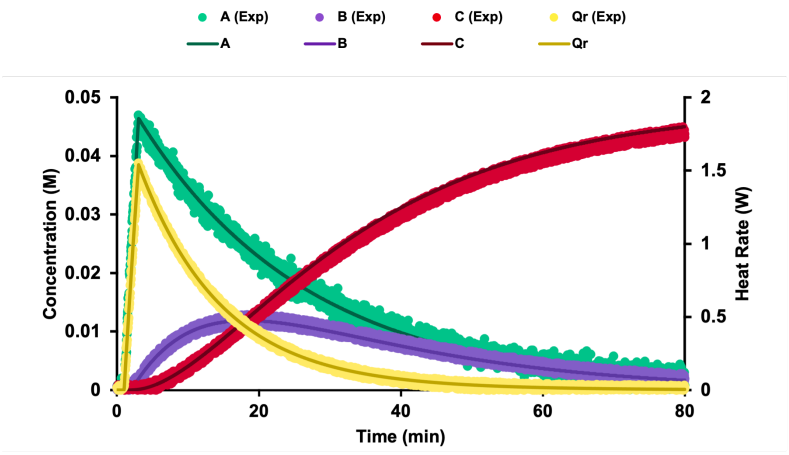

(a)

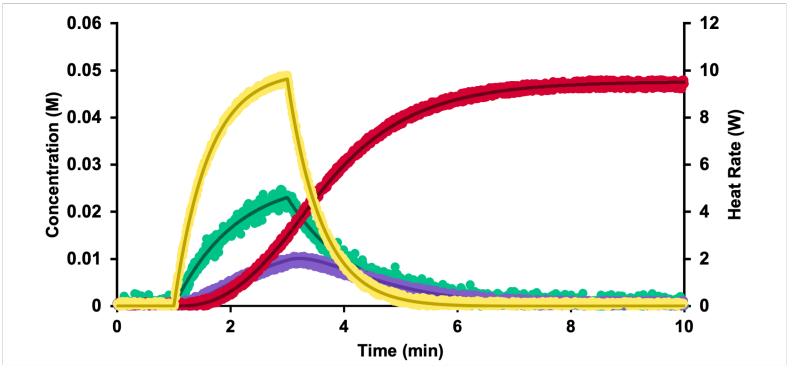

(b)

Figure 4.35: Modelling results with two experiments at two different temperatures (feed time = 2 min), stemming from 10% deviated initial iterative number, using calorimetry data and A concentration data ($\sigma = 0.02$) (a) at 25 ºC; (b) at 55 ºC.

Table 4.19: Analytical results of double experiment study: stemming from 10% deviated initial iterative numbers, using calorimetry data with or without concentration data with noise associated ($\sigma = 0.02$).

Parameter	Initial Iteration Number	Calorimetry		Calorimetry + Concentration	
		Result	Error (%)	Result	Error (%)
k_1 (min^{-1})	0.22	0.195	2.6	0.202	1.1
k_2 (min^{-1})	0.44	0.400	0.1	0.400	0.1
Ea_1 (kJ mol^{-1})	72	81.6	2.0	81.2	1.5
Ea_2 (kJ mol^{-1})	72	81.5	1.9	79.0	1.3
ΔH_{r1} (kJ mol^{-1})	-132	-123.2	2.7	-117.4	2.2
ΔH_{r2}(kJ mol^{-1})	66	63.3	5.5	57.8	3.7

The analytical outcome of the modelling experiment sustains the visual outcome (see Table 4.19). Not only the model fits the data, but also the parameters are accurately calculated (error values up to 5.5%). As previously verified, the accuracy error lowers by adding the concentration data to the modelling experiment (error up to 3.7%).

Afterwords, the iterative parameter determination was taken from values 50% (II) under the correct ones (Figures 4.36 and 4.37).

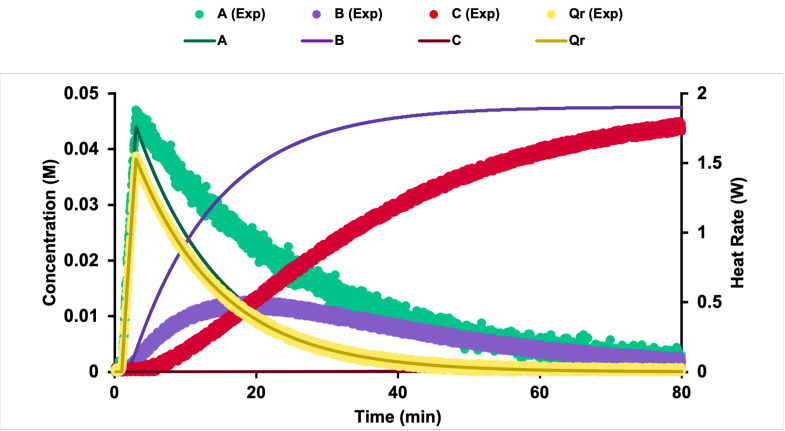

(a)

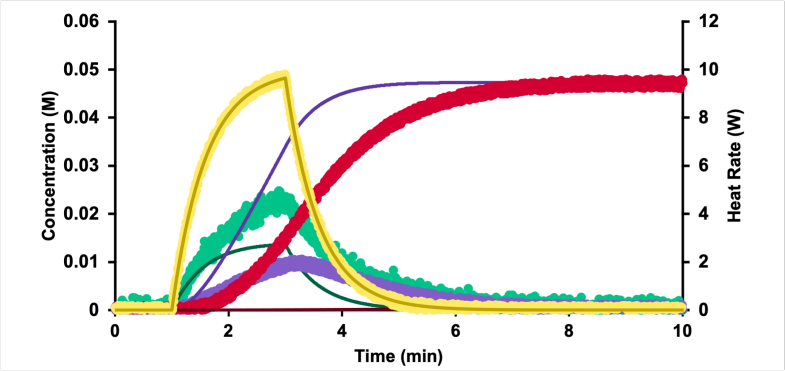

(b)

Figure 4.36: Modelling results with two experiments at two different temperatures (feed time = 2 min), stemming from 50% deviated initial iterative number, using calorimetry data ($\sigma = 0.02$) (a) at 25 ºC; (b) at 55 ºC.

According to Figure 4.36, stemming from 50% deviated initial iteration numbers, both heat profiles at two temperatures do not comprise sufficient information to accurately predict the concentration profiles.

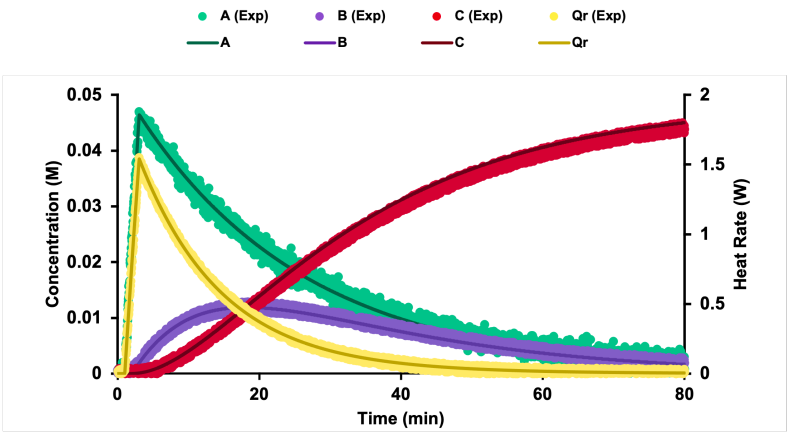

(a)

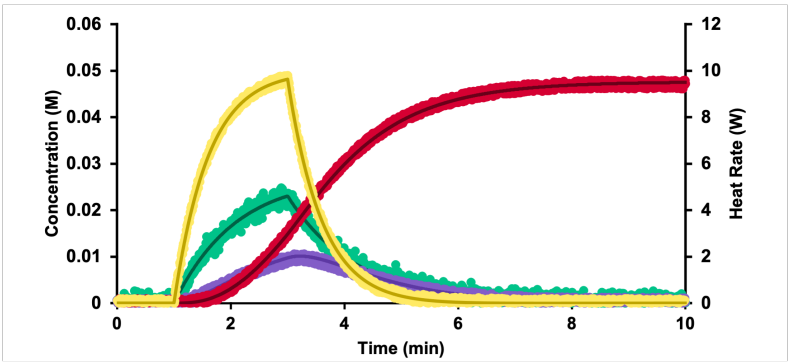

(b)

Figure 4.37: Modelling results with two experiments at two different temperatures (feed time = 2 min), stemming from 50% deviated initial iterative number, using calorimetry data and A concentration data ($\sigma = 0.02$) (a) at 25 °C; (b) at 55 °C.

Using concentration combined with the heat data and stemming from 50% deviated values, the results seem to be similar to the ones when stemming from 10% deviated values (see Figures 4.35 and 4.37).

Table 4.20: Analytical results of double experiment study: stemming from 50% deviated initial iterative numbers, using calorimetry data with or without concentration data with noise associated ($\sigma = 0.02$).

Parameter	Initial Iteration Number	Calorimetry		Calorimetry + Concentration	
		Result	Error (%)	Result	Error (%)
k_1 (min^{-1})	0.1	0.401	100.5	0.202	1.1
k_2 (min^{-1})	0.2	3.72×10^{-4}	99.9	0.400	0.2
Ea_1 (kJ mol^{-1})	40	81.7	2.1	81.2	0.1
Ea_2 (kJ mol^{-1})	40	81.9	2.1	78.9	1.3
ΔH_{r1} (kJ mol^{-1})	-60	-59.9	50.0	-117.4	2.2
ΔH_{r2}(kJ mol^{-1})	30	-3.0	105.0	57.8	3.7

While stemming from 10% deviation, the addition of A concentration profile slightly increased the accuracy of the parameters determination (Table 4.19), in this case it was determinant to obtain good results. For instance, using calorimetry only, the kinetic constants were not accurate (error around 100%) whereas using combined data the accuracy error decreases down to 1.1% (Table 4.20).

In due course, the same modelling experiments were performed from initial iteration numbers one order of magnitude below the correct parameters (90% deviated from the correct values – III, see Table 4.18). Figure 4.38 represents the outcome when only calorimetry data was used.

The Figure 4.38 show similar results to Figure 4.36. The fit of heat data was not sufficient to accurately predict the concentration profiles. Unexpectedly, when the same modelling experiment was performed using also A concentration, the model was not able to attain any result. Therefore, there is no outcome figure or any analytical results: Table 4.21 includes only modelling experiment while using calorimetry data.

Regarding the experiments using only calorimetry data, it can be concluded the model is not capable of achieving trustful results, when the kinetic and thermodynamic parameters are not well estimated before the modelling experiments ($\geq$ 50% deviation). Although, this limitation was overtaken when A concentration data was added to the fitting experiment in the first case (initial iteration number 50% distant), when stemming from 90% distant initial values, the previous was proved to become insufficient.

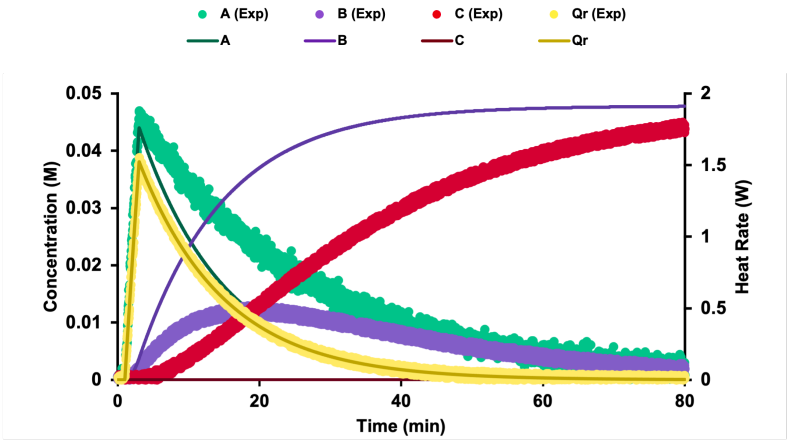

(a)

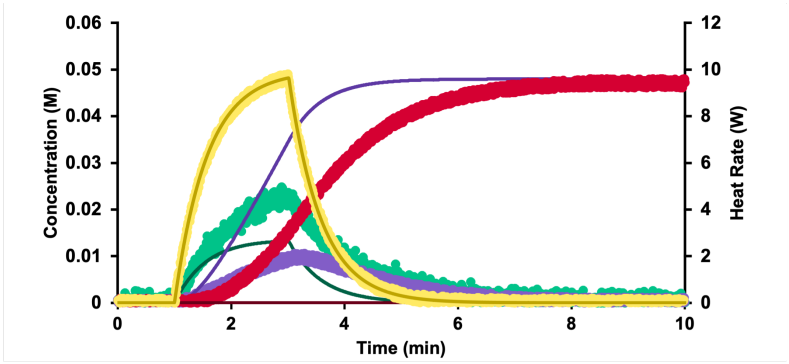

(b)

Figure 4.38: Modelling results with two experiments at two different temperatures (feed time = 2 min), stemming from 90% deviated initial iterative number, using calorimetry data ($\sigma = 0.02$) (a) at 25 ºC; (b) at 55 ºC.

Generic initial iteration values were tested ($k_i = 0.01$ min^{-1}, $Ea_i = 60$ kJ mol^{-1} and $\Delta H_{ri} = -120$ kJ mol^{-1}): Figures 4.32 and 4.33. Once more, these experiments were performed to reproduce the scenario where there is no foreknowledge on the reaction kinetics and the energy production/consumption. The corresponding analytical results are presented in Table 4.22.

Table 4.21: Analytical results of double experiment study: stemming from 90% deviated initial iterative numbers, using calorimetry data with or without concentration data with noise associated ($\sigma = 0.02$).

Parameter	Initial Iteration Number	Calorimetry		Calorimetry + Concentration	
		Result	Error (%)	Result	Error (%)
k_1 (min^{-1})	0.02	0.409	104.45	N.D.	N.D.
k_2 (min^{-1})	0.04	0.00	100	N.D.	N.D.
Ea_1 (kJ mol^{-1})	8	82.6	3.3	N.D.	N.D.
Ea_2 (kJ mol^{-1})	8	8.0	90.0	N.D.	N.D.
ΔH_{r1} (kJ mol^{-1})	-12	-59.6	50.3	N.D.	N.D.
ΔH_{r2}(kJ mol^{-1})	6	6.0	90.0	N.D.	N.D.

N.D. - Not Determined

Table 4.22: Analytical results of double experiment study: stemming from generic initial iterative numbers, using calorimetry data with or without concentration data with noise associated ($\sigma = 0.02$).

Parameter	Initial Iteration Number	Calorimetry		Calorimetry + Concentration	
		Result	Error (%)	Result	Error (%)
k_1 (min^{-1})	0.01	0.408	103.7	0.231	15.5
k_2 (min^{-1})	0.01	3.06×10^{-5}	100.0	0	100.0
Ea_1 (kJ mol^{-1})	60	82	3.0	81.7	2.1
Ea_2 (kJ mol^{-1})	60	60	25.0	60	25.0
ΔH_{r1} (kJ mol^{-1})	-120	-60	50.2	-70	41.1
ΔH_{r2}(kJ mol^{-1})	-120	-120	300.0	-120	300.0

Overall, these results show no accuracy on the kinetic and thermodynamic parameters. The fit of the model to the heat data (Figure 4.39) can not assure the correct determination of the parameters (accuracy error up to 300%). In fact, the parameters which have minor error values associated are calculated from closer initial iterative values (Ea_i and ΔH_{r1}), and that is consequence of a coincidence. When A concentration is added to the fitting window, it produces a slight improvement on the first step corresponding parameters determination, as expected.

Although, this is not a recommended practice, sometimes it is applied. This study shows that reagent concentration and heat profiles of two experiments at two different temperatures do not comprise sufficient information for modelling from generic values.

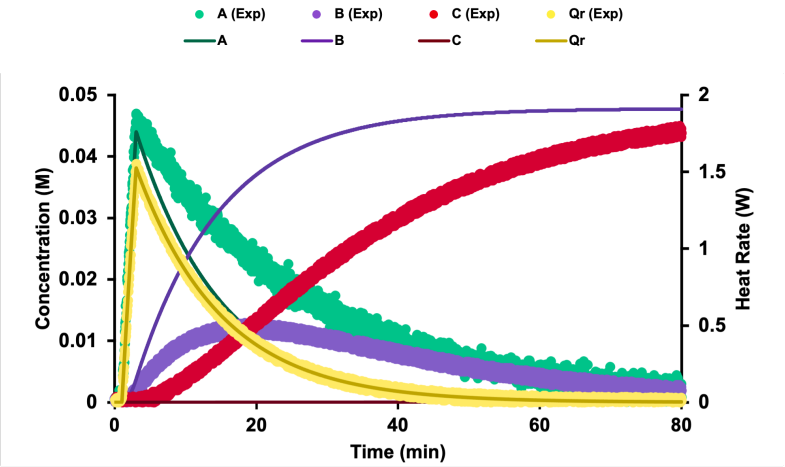

(a)

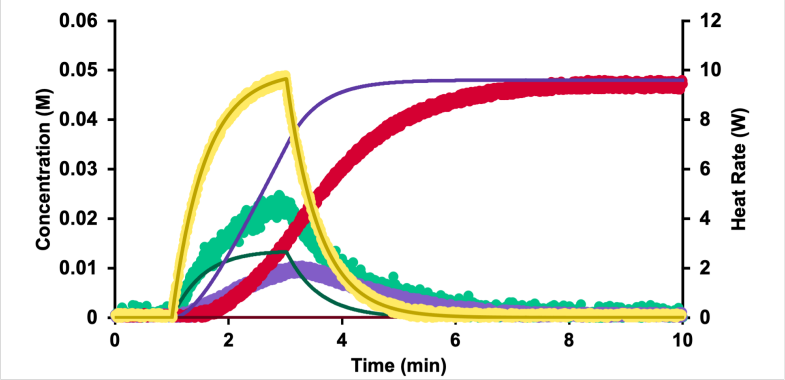

(b)

Figure 4.39: Modelling results with two experiments at two different temperatures (feed time = 2 min), stemming from generic values, using calorimetry data ($\sigma = 0.02$) (a) at 25 ºC; (b) at 55 ºC.

4.2.1 Concentration data: Discrete vs Continuous Data

Although concentration profiles provided by on-line analytical techniques are useful data in kinetic and thermodynamic parameters determination, these tools are not always available (see 1.2). Additionally, since these techniques are based on electromagnetic radiation detection, not all species are identifiable through the spectroscopic probes.

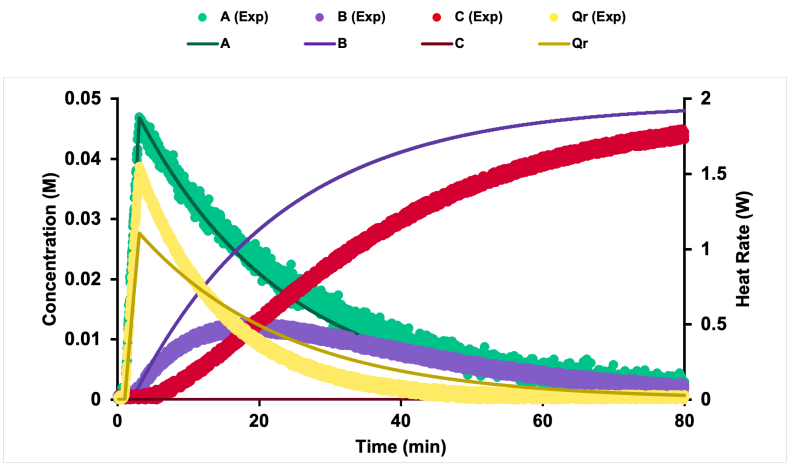

(a)

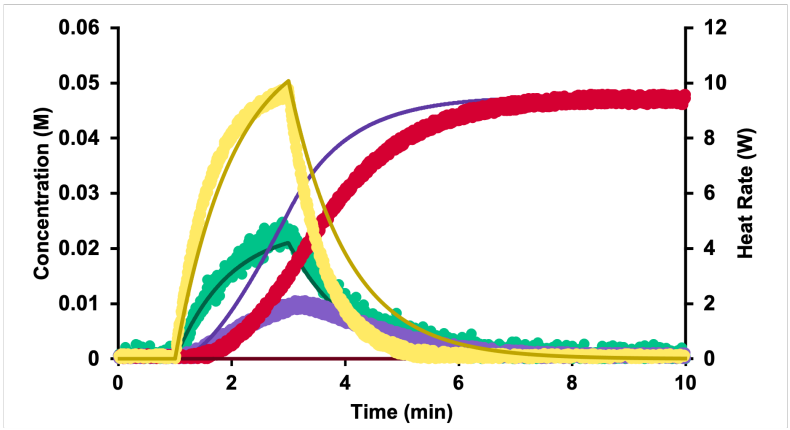

(b)

Figure 4.40: Modelling results with two experiments at two different temperatures (feed time = 2 min), stemming from generic values, using calorimetry data and A concentration data ($\sigma = 0.02$) (a) at 25 ºC; (b) at 55 ºC.

Alternatively, off-line classical methods are widely used in pharmaceutical industry to monitor the reaction, (see 1.2). In order to simulate off-line sampling, discrete concentration data was used: 6 concentration points instead of 3201 (experiment at 25 °C) and 4 points instead of 5455 (experiment at 55 °C). In this section, the results from simulated off-line sampling are presented, along with the results using concentration full profiles, in the same conditions.

To that end, two of the standard initial iteration number sets previously used were tested in the this brief study (I,V). Note, the noise associated to the data is the same and described by $\sigma = 0.02$.

Firstly, the parameters calculation was taken from 10% deviated initial values – I Table 4.18.

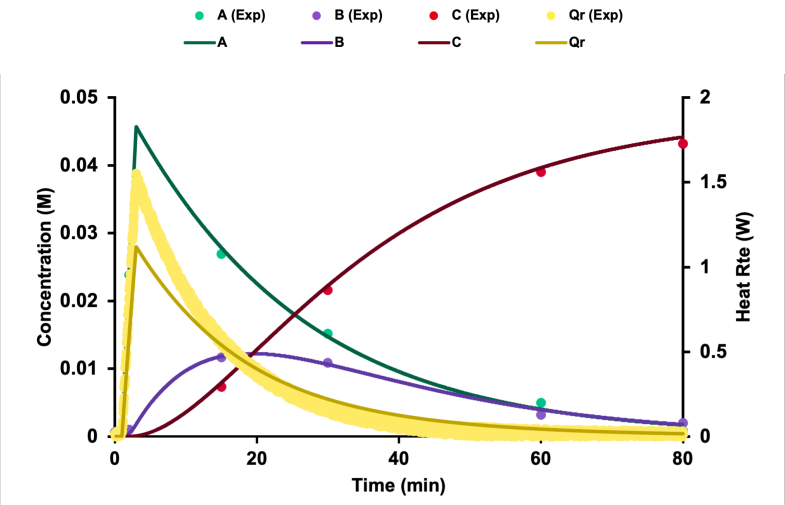

(a)

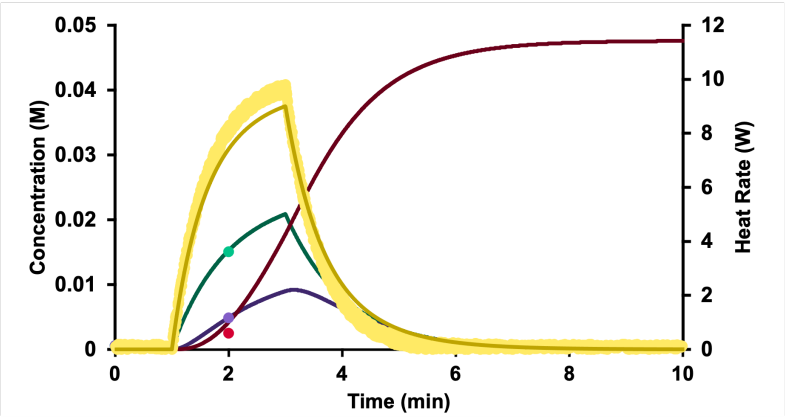

(b)

Figure 4.41: Modelling results with two experiments at two different temperatures (feed time = 2 min), stemming from 10% deviated values, using calorimetry data and concentration sampling ($\sigma = 0.02$) (a) at 25 ºC; (b) at 55 ºC.

According to Figure 4.41 it is possible to verify the fit of model to the calorimetry data is not 100% accurate, though the fit to the concentration seems right.

Table 4.23 presents the previous simulation analytical results and their respective accuracy error values, against the analytical results from the simulated probes study.

Note the previous study has taken into account only one concentration profile (reagent A), in opposition to this one with concentration sampling of three different species: reagent A, intermediate B and product C.

Table 4.23: Analytical results of double experiment study: stemming from 10% deviated initial iterative numbers, using calorimetry data with concentration samples against calorimetry and concentration profiles, with noise associated ($\sigma = 0.02$).

Parameter	Initial Iteration Number	Concentration Samples		Concentration Profile	
		Result	Error (%)	Result	Error (%)
k_1 (min^{-1})	0.22	0.228	14.0	0.202	1.1
k_2 (min^{-1})	0.44	0.443	10.7	0.400	0.1
Ea_1 (kJ mol^{-1})	72	88.3	10.4	81.2	1.5
Ea_2 (kJ mol^{-1})	72	89.3	11.6	79.0	1.3
ΔH_{r1} (kJ mol^{-1})	-132	-88.8	26.0	-117.4	2.2
ΔH_{r2}(kJ mol^{-1})	66	28.3	52.9	57.8	3.7

Even though the three species were taken into the simulation, the results are more accurate while only A concentration complete profile was used: 14.6 in opposition to 1.1% (k_1), 10.7 in opposition to 0.1% (k_2), 10.4 in opposition to 1.5% (Ea_1), 11.6 in opposition to 1.3 % (Ea_2), 26.0 in opposition to 2.2% (ΔH_{r1}) and 52.9 in opposition to 3.7% (ΔH_{r2}). As expected, the use of continuous on-line concentration data implies significant improvement on the accuracy of the results, over discrete sampling. This type of data improves not only the accuracy of the results, as it would save time on the parameters determination process: at the experimental stage and at the modelling stage.

Afterwards, the generic initial iteration values were tested – V, Table 4.18. Figure 4.42 represents the visual outcome of the simulation, while Table 4.24 represents sampling against progress analytical results.

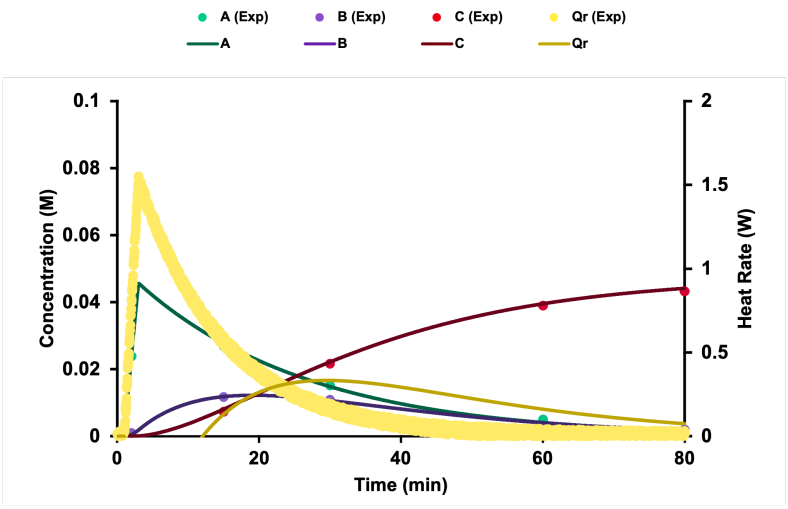

(a)

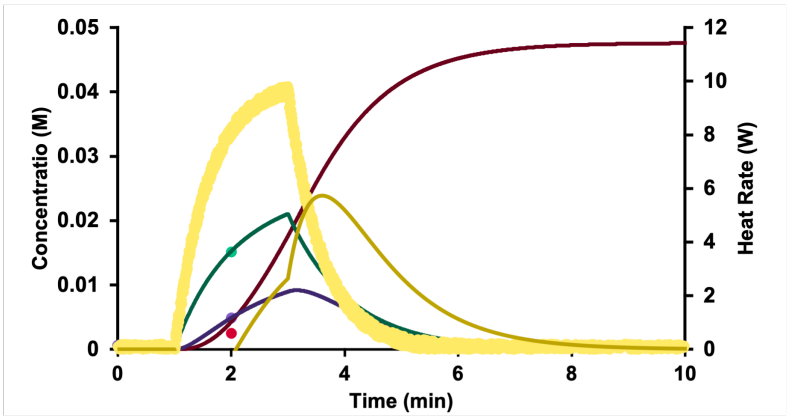

(b)

Figure 4.42: Modelling results with two experiments at two different temperatures (feed time = 2 min), stemming from generic values, using calorimetry data and concentration sampling ($\sigma = 0.02$) (a) at 25 ºC; (b) at 55 ºC.

Stemming from generic values, the difference between the accuracy error is smaller, since the results using probes were not satisfactory (error up to 300%). The addition of data about B and C has favored the estimation of the second step kinetic parameters with reasonable margin (up to 18%).

Regarding the thermodynamic parameters, the accuracy is still not acceptable (error up to 279%). These results sustain the previous conclusion: the data should be analysed before modelling. Nevertheless, this estimation becomes harder with less data.

Table 4.24: Analytical results of double experiment study: stemming from generic initial iterative numbers, using calorimetry data with concentration samples against calorimetry and concentration profiles, with noise associated ($\sigma = 0.02$).

Parameter	Initial Iteration Number	Concentration Samples		Concentration Profile	
		Result	Error (%)	Result	Error (%)
k_1 (min^{-1})	0.01	0.235	17.6	0.231	15.5
k_2 (min^{-1})	0.01	0.459	14.8	0	100.0
Ea_1 (kJ mol^{-1})	60	82	9.4	81.7	2.1
Ea_2 (kJ mol^{-1})	60	88.6	10.7	60.0	25.0
ΔH_{r1} (kJ mol^{-1})	-120	71.2	159.4	-70.6	41.1
ΔH_{r2}(kJ mol^{-1})	-120	-107.3	278.9	-120.0	299.9

Overall, this brief study comparing discrete with continuous data shows the improvement on the results when using spectroscopic probes over discontinuous off-line HPLC samples, for instance. Even though these study compares 1 concentration profile with 3 sample sets, the results are leaning on the progress techniques. In fact, the on-line techniques are more expedite and allow one to follow the reaction in real time and without sampling. Additionally, when there is more points, as in this case, possibly the noise becomes more insignificant on the calculation results. However, as already been referred, not all species are identifiable through spectroscopic probes and it is different from technique to techniques, depending on the radiation detected. The detected radiation depends on the functional groups which may or not be present on the studied system.

On another hand, it would be possible to increase the number of samples taken during the reaction. In fact, in the future, it would be interesting to test this approach with different sample quantities to find the minimum samples required according to different initial iteration numbers. However, one should bare in mind off-line sampling and data treatment are more laborious.

5

Conclusion and Recommendations

The scope of this work was the chemical development on pharmaceutical industry and the main goal was to include calorimetry data in the kinetic modelling of chemical reactions. Two approaches to this issue were presented in this work.

The first consisting in a case study: acetic anhydride hydrolysis, a widely studied reaction concerning calorimetric studies. The first-order one step model was validated with experimental data of a reaction calorimeter and on-line FTIR concentration derived data. Three isothermal experiments were used to estimate the exponential factor, the activation energy and the reaction enthalpy. The final results were in agreement with the literature results. It was concluded that for a fist-order single step reaction, the 3 combined experiments provided successful results. Besides, it was demonstrated the potential of the results, by predicting a scale up operation in optimal conditions. Further development on this study could be the validation of the optimized scenario in the manufacturing unit.

Following the case study example, a slightly more complex reaction was subject of an systematic study: two-step consecutive reaction. The approach consisted in comparing the calorimetric data only derived results with calorimetric combined with on-line concentration derived results. To that end, different initial iteration values were used.

During this study, single isothermal experiments with different associated noises were used to compare the impact of the noise in the results. Both models (one built during this work and the DC model) were able to converge to acceptable results, even with the noise associated. However, the data used for the modelling experiments comprised 3021 for each data set. It would be interesting to compare this results with a similar modelling experiment yet using less points, to understand if the impact of the noise would increase with decreasing data quantity. Additionally, it was verified that without the concentration profiles the results are not descriptive as needed, in order to cover the lack of information on the reactions systems.

The modelling experiments using two isothermal experiments is more faithful to the reality, in which all the parameters need to be estimated, so at least two runs at two temperatures have to be performed. This study proved the modelling experiments should be done after some previous knowledge on the reaction, having in mind the chemical behaviour of the species at hand. Chemical principles can not be left out of the modelling experiment. Pre-fitting the data is more recommended than the iterative process of estimating the kinetic and thermodynamic parameters. For this it could be used a molecular modelling tool [34]. This study conclusion corroborated the previous ones: the concentration data is important for a faster and more accurate parameter determination, therefore, chemical development. In fact, the calorimetry data has the limitation of not differentiating the heat sources, which is complemented with the concentration data. On another hand, the concentration based measurements do not give information on the energy associated to the chemical phenomena. This information is crucial for safe and optimal scale-up, as explained in 1.
The systematic study approach was revealed to be a convenient tool to address the methodology issue, without experimentation. Nevertheless, it would be useful to take this study further, for instance, to address different $\frac{k_2}{k_1}$ or different magnitudes of the heat released/consumed at each step.

On the other hand, to some extent the studied reaction has a simple mechanism. It would be interesting to address different, gradually more complex mechanisms. Probably, with increasingly complex systems, increasingly experimentation and/or data would be needed. The generator constructed during this work would allow this study to be extended to other mechanisms, by simply changing the kinetic rate law, for instance, more steps involved on the kinetics or parallel mechanisms instead of consecutive and so on.

Regarding the comparison study between the discrete samples (simulating off-line samples, widely used in pharmaceutical Industry – see **??**) and progress based measurements, for a more descriptive knowledge and faster development, the progress techniques were concluded to be a better suited analytical technique. For that reason, they are already being used, for progress kinetic modelling, as described in **??**.

It could be also explored a thermal dynamic operation instead of only isothermal essays. It would increase the complexity of the model, however it would decrease the number of experiments.

It is worth to highlight that even though this work was focused on core of the reaction, the methodology of safe and optimal scale up based on the reaction kinetics and thermodynamics should include the reactor heat transfer characterization and its scale up prediction, as demonstrated.

The aims of the thesis were globally achieved: recommendations for the methodology were extracted of this study, contributing to a QbD approach. Nevertheless, more studies should be conducted to widen the conclusions to more other reactions.

Bibliography

[1] A. Zogg, "A combined approach using calorimetry and IR-ATR spectroscopy for the determination of kinetic and thermodynamic reaction parameters," Ph.D. dissertation, Swiss Federal Institute of Technology Zurich, 2003. [Online]. Available: https://doi.org/10.3929/ethz-a-010025751

[2] A. C. Dimian, C. S. Bildea, and A. A. Kiss, "Integrated Process and Product Design," in Computer Aided Chemical Engineering, 2014, vol. 35, pp. 1–33. [Online]. Available: https://linkinghub.elsevier.com/retrieve/pii/B9780444627001000012

[3] G. E. Rotstein, L. G. Papageorgiou, N. Shah, D. C. Murphy, and R. Mustafa, "A Product Portfolio Approach in the Pharmaceutical Industry," Computers and Chemical Engineering, vol. 23, no. SUPPL. 1, pp. 5883–5886, 1999.

[4] D. J. A. Ende, "Chemical Engineering in Pharmaceutical Industry: An Introduction," in Chemical Engineering in the Pharmaceutical Industry: R&D to Manufacturing, 1st ed., D. J. A. Ende, Ed. Wiley, 3 2011, ch. 1, pp. 3–21. [Online]. Available: https://onlinelibrary.wiley.com/doi/book/10.1002/9781119600800

[5] FDA, "Guidance for Industry, PAT-A Framework for Innovative Pharmaceutical Development, Manufacturing and Quality Assurance," 2004. [Online]. Available: http://www.fda.gov/downloads/Drugs/GuidanceComplianceRegulatoryInformation/Guidances/ucm070305.pdf

[6] A. J. Hickey, "Quality Principles," in Pharmaceutical Process Engineering, 2nd ed., A. J. Hickey and D. Ganderton, Eds. New York: Informa Healthcare, 2010, vol. 195, ch. 17, pp. 193–205.

[7] G. M. Troup and C. Georgakis, "Process systems engineering tools in the pharmaceutical industry," Computers and Chemical Engineering, vol. 51, pp. 157–171, 2013. [Online]. Available: http://dx.doi.org/10.1016/j.compchemeng.2012.06.014

[8] P. Haines, "The Reasons for Using Thermal and Calorimetric Methods," in Principles of Thermal Analysis and Calorimetry. Cambridge: The Royal Society of Chemistry, 2002, ch. Introducti, p. 6.

[9] S. I. Gianoli, G. Puxty, U. Fisher, M. Maeder, and K. Hungerbühler, "Empirical kinetic modeling of on line simultaneous infrared and calorimetric measurement using a Pareto optimal approach and multi-objective genetic algorithm," Chemometrics and Intelligent Laboratory Systems, vol. 85, no. 1, pp. 47–62, 2007.

[10] A. Zogg, U. Fischer, and K. Hungerbühler, "A new approach for a combined evaluation of calorimetric and online infrared data to identify kinetic and thermodynamic parameters of a chemical reaction," Chemometrics and Intelligent Laboratory Systems, vol. 71, no. 2, pp. 165–176, 2004.

[11] A. Zogg, F. Stoessel, U. Fischer, and K. Hungerbühler, "Isothermal reaction calorimetry as a tool for kinetic analysis," Thermochimica Acta, vol. 419, no. 1-2, pp. 1–17, 9 2004. [Online]. Available: https://linkinghub.elsevier.com/retrieve/pii/S0040603104000486

[12] E. A. Garcia-Hernandez, C. R. Souza, L. Vernières-Hassimi, and S. Leveneur, "Kinetic modeling using temperature as an on-line measurement: Application to the hydrolysis of acetic anhydride, a revisited kinetic model," Thermochimica Acta, vol. 682, no. August, p. 178409, 12 2019. [Online]. Available: https://doi.org/10.1016/j.tca.2019.178409https://linkinghub.elsevier.com/retrieve/pii/S0040603119306422

[13] L. Guldbæk Karlsen and J. Villadsen, "Isothermal reaction calorimeters—I. A literature review," Chemical Engineering Science, vol. 42, no. 5, pp. 1153–1164, 1987. [Online]. Available: https://linkinghub.elsevier.com/retrieve/pii/0009250987800659

[14] W. Regenass, "The development of heat flow calorimetry* as a tool for process optimisation and proof, safety Available calorimetric principles / classification of calorimetric instruments," vol. 49, pp. 1661–1675, 1997.

[15] R. André, M. Giordano, C. Mathonat, and R. Naumann, "A new reaction calorimeter and calorimetric tools for safety testing at laboratory scale," Thermochimica Acta, vol. 405, no. 1, pp. 43–50, 10 2003. [Online]. Available: https://linkinghub.elsevier.com/retrieve/pii/S0040603103001291

[16] Z.-C. Guo, W.-S. Bai, Y.-J. Chen, R. Wang, L. Hao, and H.-Y. Wei, "An adiabatic criterion for runaway detection in semibatch reactors," Chemical Engineering Journal, vol. 288, pp. 50–58, 3 2016. [Online]. Available: http://dx.doi.org/10.1016/j.cej.2015.11.065https://linkinghub.elsevier.com/retrieve/pii/S1385894715016174

[17] R. N. Landau, "Expanding the role of reaction calorimetry," Thermochimica Acta, vol. 289, no. 2, pp. 101–126, 1996.

[18] U. K. Singh and C. J. Orella, "Reaction Kinetics and Characterization," in Chemical Engineering in the Pharmaceutical Industry: R&D to Manufacturing, 1st ed., D. A. Ende, Ed. New Jersey, USA: John Wiley & Sons, Ltd, 2011, ch. 7, pp. 79–99.

[19] W. L. Luyben, "Fundamentals," in Process Modeling,simulation and control for chemical engineers, 2nd ed., W. L. Luyben, Ed. New York: McGraw-Hill, 1996, ch. 2, pp. 15–38.

[20] N. C. Imlinger, C. Blattner, M. Krell, and M. R. Buchmeiser, "Hard-modeling of reaction kinetics by combining online spectroscopy and calorimetry," Journal of Chemometrics, vol. 22, no. 11-12, pp. 758–767, 11 2008. [Online]. Available: http://doi.wiley.com/10.1002/cem.1196

[21] D. G. Blackmond, "Reaction progress kinetic analysis: A powerful methodology for mechanistic studies of complex catalytic reactions," Angewandte Chemie - International Edition, vol. 44, no. 28, pp. 4302–4320, 2005.

[22] R. N. Landau, D. G. Blackmond, and H. H. Tung, "Calorimetric Investigation of an Exothermic Reaction: Kinetic and Heat Flow Modeling," Industrial and Engineering Chemistry Research, vol. 33, no. 4, pp. 814–820, 1994.

[23] F. Stoessel and O. Ubrich, "Safety assessment and optimization of semi-batch reactions by calorimetry," Journal of Thermal Analysis and Calorimetry, vol. 64, no. 1, pp. 61–74, 2001.

[24] C. Guinand, M. Dabros, T. Meyer, and F. Stoessel, "Reactor dynamics investigation based on calorimetric data," Canadian Journal of Chemical Engineering, vol. 95, no. 2, pp. 231–240, 2017.

[25] M. C. Maier, M. Leitner, C. O. Kappe, and H. Gruber-Woelfler, "A modular 3D printed isothermal heat flow calorimeter for reaction calorimetry in continuous flow," Reaction Chemistry & Engineering, vol. 5, no. 8, pp. 1410–1420, 2020. [Online]. Available: http://xlink.rsc.org/?DOI=D0RE00122H

[26] M. Eissen, A. Zogg, and K. Hungerbühler, "The runaway scenario in the assessment of thermal safety: Simple experimental access by means of the catalytic decomposition of H2O2," Journal of Loss Prevention in the Process Industries, vol. 16, no. 4, pp. 289–296, 2003.

[27] P. Lerena, W. Wehner, H. Weber, and F. Stoessel, "Assessment of hazards linked to accumulation in semi-batch reactors," Thermochimica Acta, vol. 289, no. 2, pp. 127–142, 1996.

[28] F. Stoessel, "Semi-batch Reactors," in Thermal Safety of Chemical Processes, 2008, pp. 147–178.

[29] Mettler Toledo, "Reaction Calorimeter - Chemical Process Safety." [Online]. Available: www.mt.com/RC1mx

[30] K. J. P. Orton and M. Jones, "Hydrolysis of acetic anhydride," J. Chem. Soc., Trans., vol. 101, no. 0, pp. 1708–1720, 1 1912. [Online]. Available: https://pubs.rsc.org/en/content/articlehtml/1912/ct/ct9120101708https://pubs.rsc.org/en/content/articlelanding/1912/ct/ct9120101708http://xlink.rsc.org/?DOI=CT9120101708

[31] W. H. Hirota, R. B. Rodrigues, C. Sayer, and R. Giudici, "Hydrolysis of acetic anhydride: Non-adiabatic calorimetric determination of kinetics and heat exchange," Chemical Engineering Science, vol. 65, no. 12, pp. 3849–3858, 6 2010. [Online]. Available: https://linkinghub.elsevier.com/retrieve/pii/S0009250910001764

[32] F. Susanne, D. S. Smith, and A. Codina, "Kinetic Understanding Using NMR Reaction Profiling," Organic Process Research & Development, vol. 16, no. 1, pp. 61–64, 1 2012. [Online]. Available: https://pubs.acs.org/doi/10.1021/op200202k

[33] S. Asprey, B. Wojciechowski, N. Rice, and A. Dorcas, "Applications of temperature scanning in kinetic investigations: The hydrolysis of acetic anhydride," Chemical Engineering Science, vol. 51, no. 20, pp. 4681–4692, 10 1996. [Online]. Available: https://linkinghub.elsevier.com/retrieve/pii/0009250996003065

[34] M. Döntgen, F. Schmalz, W. A. Kopp, L. C. Kröger, and K. Leonhard, "Automated Chemical Kinetic Modeling via Hybrid Reactive Molecular Dynamics and Quantum Chemistry Simulations," Journal of Chemical Information and Modeling, vol. 58, no. 7, pp. 1343–1355, 2018.